UNIVERSITÀ
DEGLI STUDI
DI PADOVA

Head Office: Università degli Studi di Padova

Department: Scienze del Farmaco

Ph.D. COURSE IN: MOLECULAR SCIENCES
CURRICULUM: PHARMACEUTICAL SCIENCES
SERIES: 30

ORGANIC SELENIUM COMPOUNDS AS OXIDANTS IN CANCER THERAPY

(Thesis written with the financial contribution of Fondazione Cariparo)

Coordinator: Prof. Leonard Prins
Supervisor: Prof. Valentina Gandin
Co-Supervisor: Prof. Aristi Fernandes

Ph.D. student: Jeremy Braude

Acknowledgments

To my parents, Gary and Sharon, my siblings, Laurence, Daniella and Madison, my girlfriend, Molly, and all my family and friends,

For all of your love and support.

To my supervisor, Valentina, and to all my colleagues over the past 3 years,

For their part in my great Italian adventure.

Contents

1 Introduction

1.1 Selenium Chemistry

Selenium (Se) is a non-metal chemical element with atomic number 34. It displays chemical properties that are intermediate between sulphur and tellurium, which are found directly above and below Se on the periodic table, respectively. Se has an atomic radius of 120pm and its electronic configuration is [Ar] $4s^2$ $3d^{10}$ $4p^4$. Se is rarely found in its elemental state in nature, while it is more commonly found in metal sulphide ores, where it can replace sulphur. Se compounds are typically found in the oxidation states +6,+ 4,+ 2 and -2. In its elemental state, Se exists in two forms, as a red powder and as a silvery metal.

1.2 Selenium in Human Health

The balance of Se in the body is critical to human health. Deficits in Se can lead to severe neurological, cardiovascular and immunological disorders, as well as an increased risk of developing cancer, while excess Se results in toxicity[1]. To maintain a selenium balance of zero (whereby selenium intake equals selenium excretion), the required dietary Se intake is approximately 55-80 µg/day. Interestingly, there are large-scale differences between the mean intake of Se across continents, with North Americans taking in 90-130 µg (Se) per day and Europeans taking in about 40 µg (Se) per day[1]. The range for optimal Se intake is quite narrow, with toxic effects (selenosis) having been observed at intake levels as low as 400 µg per day.

Se flows through the food chain from soil to plants and then to animals and humans. The Se used by the human body is acquired in the diet and includes a variety of species, including selenite, selenate, selenocysteine and selenomethionine. In general, selenate is the major inorganic form of dietary Se, found in both animal and plant tissues, while selenomethionine is the major organic form of dietary Se, found in cereal grains, legumes and soybeans, and meat, as well as in Se-enriched yeast used for supplementation. Importantly, in human and mouse studies, the bioavailability of selenomethionine was shown to be greater than that of both selenite and selenate and is likely to be the main source of Se for mammals[1,2].

The Se content of food is largely dependent on soil Se content, which can vary from being extremely toxic to livestock to being extremely low and the cause of human Se deficiency[1]. In fact, the amount of whole-body Se found in adult humans was reported to differ in different countries, due to the uneven geographic distribution of Se in soil. Moreover, the distribution of Se in the human body is determined by its availability. Under normal dietary conditions, the highest Se concentration is detected in kidney, followed by liver, spleen, pancreas, heart, brain, lung, bone and skeletal muscle. However, when Se intake is insufficient, its distribution changes according to the priority of different organs for Se, with the brain having a notably high priority for Se retention[1].

1.3 Selenium Metabolism

Selenium (Se) is an essential trace element that exists naturally in both organic and inorganic forms. The major physiological functions of Se are exerted through the incorporation of metabolically produced selenocysteine, commonly termed the 21st amino acid, into selenoproteins. At least twenty-five human selenoproteins have been identified through genome scanning, including five glutathione peroxidases (GPx1, 2, 3, 4 and 6), three thioredoxin reductases (TrxR1, 2 and 3), three iodothyronine deiodinases (DI, II and III), selenophosphate synthetase 2, selenoprotein P, among others[3]. Sec residues are found at the active site of selenoenzymes and, although selenocysteine is structurally similar to cysteine (Cys), its incorporation into selenoenzymes is critical to their catalytic function[4,2]. This is due to Se being a better nucleophile than sulphur at physiological pH, meaning that Sec is ionized whereas Cys would be protonated[5].

Selenocysteine is a rare and unique amino acid that is encoded by the UGA “stop codon” and requires specialised molecular machinery for its translation[6]. Firstly, the selenocysteine insertion sequence (SECIS) element, a stem-loop secondary structure found in the 3’ UTR of selenoprotein mRNA, is necessary for read-through and Sec insertion at the UGA codon[7–9]. Secondly, unlike other amino acids, Sec is biosynthesised directly on its tRNA, termed tRNA$^{[Ser]Sec}$. In this process, the tRNA is initially aminoacylated with serine (by Ser-tRNA synthase) and phosphorylated (by phosphoseryl-tRNA kinase) to yield phosphoseryl-tRNA$^{[Ser]Sec}$. The phosphoseryl residue is then converted to Sec by selenocysteine synthase,

which utilises metabolically produced monoselenophosphate ($HSePO_3^{2-}$) to form Sec-tRNA$^{[Ser]Sec}$ [10]. In contrast to the process of selenoprotein synthesis, selenomethionine and Sec may be directly, but non-specifically, incorporated into proteins in place of methionine (Met) and Cys, respectively[11].

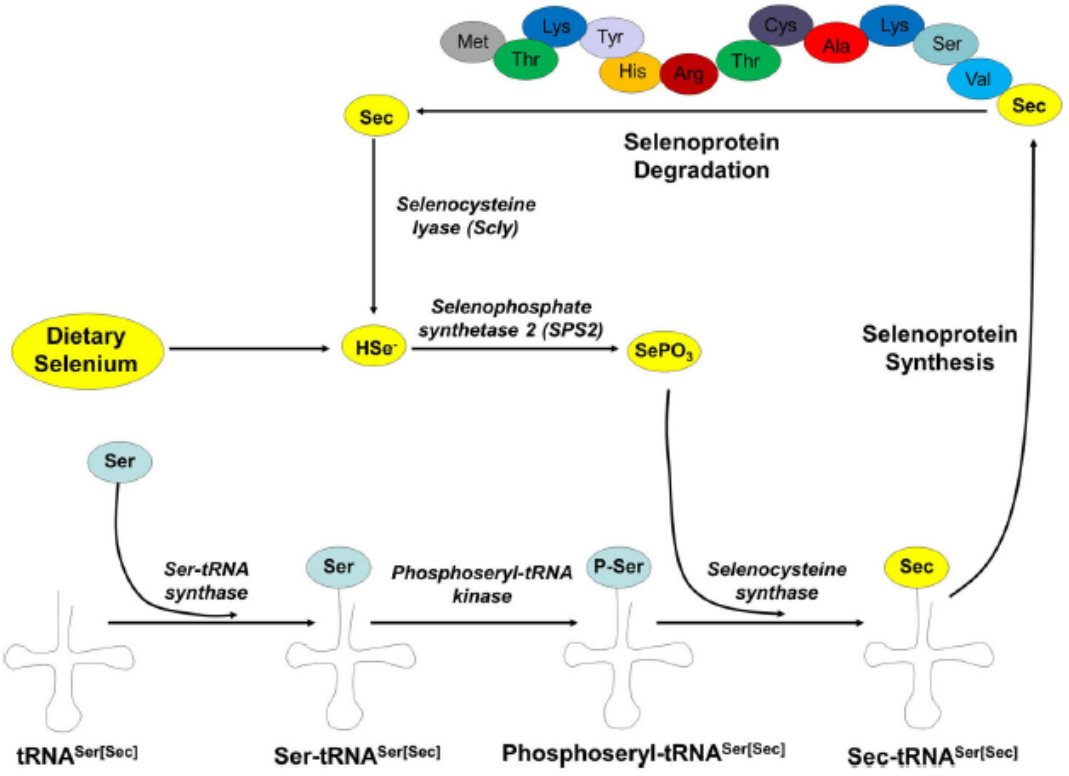

Direct biosynthesis of Sec on its tRNA molecule [12]. Sec is produced by selenocysteine synthase on a tRNA with a phosphorylated Ser (P-Ser) residue, consuming metabolically produced selenophosphate ($SePO_3$).

Dietary Se is acquired in a variety of both organic and inorganic forms. However, regardless of the Se species, dietary Se must be converted to an inorganic precursor, selenide (HSe^-), which can then be converted to selenophosphate ($HSePO_3^{2-}$) for selenoprotein synthesis [11,13]. Inorganic selenate and selenite as well as selenodiglutathione are converted to HSe^- via the reduction of thiols, which is facilitated by glutathione (GSH) and both the glutaredoxin and thioredoxin systems[14,15]. Certain organic Se compounds, on the other hand, are converted to an intermediate metabolite, methylselenol (CH_3Se^-), before being demethylated to HSe^-. Both cleavage of seleno-methylselenocyteine (MSC) by β-lyase and reduction of methylseleninic acid (MSA) produce CH_3Se^-. Dietary Sec and Sec produced

through methylation of selenomethionine (SeMet), on the other hand, are converted to HSe^- by β-lyase[13].

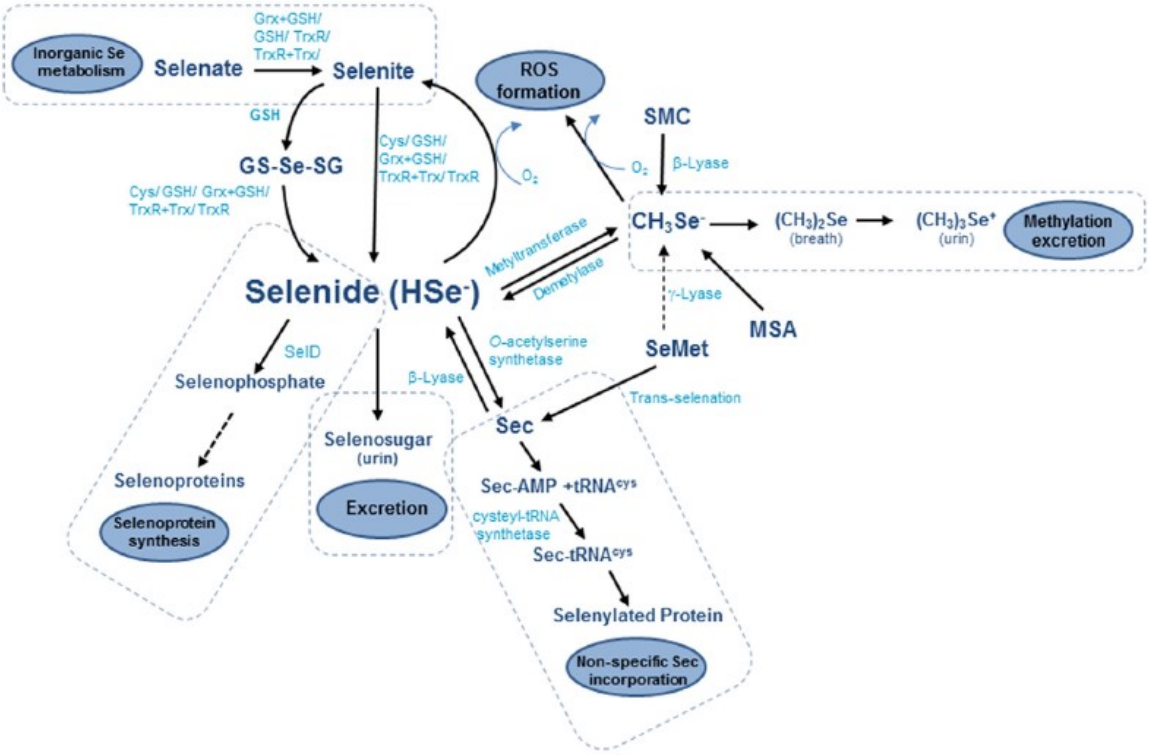

The metabolism of organic and inorganic Se molecules[13]. While inorganic Se forms, such as selenate and selenite are reduced chemically and enzymatically to form selenide, organic Se molecules form an in intermediary metabolite, methylselenol (CH_3Se^-), before being de-methylated into selenide.

1.4 Selenium and Cancer

During the past decades, the connection between selenium and cancer has been widely studied from many different aspects, ranging from its use as a tracer molecule to its use as a cancer preventative agent and, more recently, its use as a cancer therapeutic agent. Epidemiological studies have revealed lower death rates due to cancer in regions characterized by higher levels of Se in the soil, and a correlation between the occurrence of certain types of cancer and plasma Se levels [16–18]. Although the potential of Se derivatives as cancer preventing agents has been examined since the 80's, more recent studies have focused on Se derivatives as attractive therapeutic agents for the treatment of

aggressive/advanced neoplasias. In addition, Se supplementation in patients receiving conventional anticancer therapies has been shown to enhance treatment efficacy, limit side effects, and improve general patient condition[19–21]

Se compounds have become interesting anti-tumour agents with mounting reports over the past decades demonstrating their high efficacy and selectivity toward cancer cells[13]. Since inorganic and organic Se compounds are metabolized differently in vivo, they activate distinct molecular mechanisms and exhibit varying degrees of toxicity and anticancer activity[22]. Inorganic Se forms generally exhibit genotoxic effects, which in turn may account for a lower therapeutic window, a higher systemic toxicity, and an increased risk of second malignancy occurrence in treated patients. Conversely, organic Se compounds, in addition to retaining a significant antitumor activity with an increased ability to prevent metastasis, also have fewer side effects and minimal or no genotoxic potential[23,24].

1.4.1 Increasing Oxidative Stress to Target Cancer Cells

Redox homeostasis is critical for maintaining regular physiological functions and ensuring cell survival. The regulation of intracellular reactive oxygen species (ROS) levels is therefore crucial for upholding homeostasis. At low to moderate levels, ROS have the physiological role of acting as signalling molecules that sustain cellular proliferation, differentiation and survival. H_2O_2 for instance, can serve as a signal for proliferation, differentiation as well as migration, but can also act as a signal transduction molecule that can induce pro-inflammatory cytokines and the nuclear factor-kB. At higher levels, ROS can impair cellular redox homeostasis, generating oxidative stress that can result in DNA damage, irreversible protein oxidation, and lipid peroxidation. In order to regulate ROS levels, cells scavenge

ROS both chemically, by free thiols and other antioxidant molecules, and enzymatically, via reduction reactions in the mitochondria and cytosol by superoxide dismutase, the thioredoxin and glutaredoxin systems, glutathione reductase and glutathione peroxidase, among other enzymes.

Although cellular transformation during carcinogenesis arises from many different pathways, the metabolic requirements of different tumour cells are generally believed to be similar[25]. One of the central requirements is to counteract the increase in oxidizing effects that arise from the aberrant metabolism of transformed cells, as well as the increase in ROS

production. This is achieved through the induction of antioxidant scavenging molecules. Consequently, while healthy cells are characterized by a low steady-state level of ROS and reducing equivalents, transformed cells possess increased levels of ROS and reducing equivalents. Cancer cells display accelerated aerobic glycolysis (the Warburg effect) and increased dependence on the pentose phosphate cycle, which facilitates their uncontrolled growth and accounts for their excess production of ROS. To counteract oxidative stress, cancer cells must up-regulate ROS scavenging mechanisms, which leaves little or no room for further adaptation to the induction of additional oxidative stress. Hence, targeting the consumption or inhibition of antioxidant systems, may specifically disrupt redox balance in cancer cells, leading to the generation of oxidative stress and ultimately cell death. Specifically, inducing oxidative stress may lead to the preferential killing of cancer cells, since cancer cells are likely to be more sensitive than normal cells, thus offering a therapeutic window for treatment[26,27].

Regarding the induction of oxidative stress in cancer cells by treatment with oxidants, Se compounds are very interesting candidates. As redox modulators, many Se compounds have shown beneficial properties and have gained substantial attention. Moreover, many new compounds are currently being designed, synthesized and evaluated for their efficacy and specificity as anticancer agents. As of now, organic Se compounds have proved to be more promising than inorganic compounds; however, more studies are required to evaluate their effects on cancer cell metabolism.

1.4.2 Selenium Compounds as Cytotoxic Agents: Oxidative Stress and Selective Uptake

Since tumour cells are generally more vulnerable to induced oxidative stress, they have also proven to be more susceptible to Se compounds[28–30]. Importantly, the cytotoxic effects of Se compounds have been observed at pharmacologically achievable doses, offering a therapeutic window for the use of Se compounds as anticancer agents. There is a variety of mechanisms underlying the anticancer properties of Se compounds, which vary according to the dose, chemical structure, redox state and experimental model used[31]. Once inside the cell, Se compounds can undergo redox reactions and change both their form and oxidation state, producing different metabolites, such as hydrogen selenide (HSe-) and methylselenol (CH_3Se-) in response to the cellular environment[32]. These redox active Se metabolites are

highly nucleophilic and are therefore very reactive, rendering them efficient anticancer agents.

The main mechanism by which these compounds generate ROS in cancer cells is by redox cycling of selenolates with the aforementioned chemical and enzymatic antioxidant systems, resulting in the production of superoxide and hydrogen peroxide. In addition, Se compounds can also directly interact with free thiols and selenols, and cause the oxidation of proteins, other biomacromolecules, and low molecular weight compounds. In proteins, for example, these reactions result in the formation of intra- or inter- molecular bonds, including selenotrisulfides bonds (S-Se-S), selenenylsulfide bonds (Se-S), and diselenide bonds (Se-Se) [33]. The redox active Se compounds may also catalyse the formation of disulfide bonds (S-S) and/or mixed disulfide bonds with glutathione (S-SG) or nitric oxide (S-NO). These oxidations can result both in downstream biological effects and in direct effects on the structure, function or activity of proteins. Direct modification and regulation of signalling proteins through thiol oxidation are known to impact protein kinases, phosphatases, and transcription factors[34]. Among those that have been best characterized are caspases, p53, Jun, AP-1, APE-1/Ref-1, Sp1, NF-κB, ASK-1 and JNK [35–38]. Ultimately, redox modification of thiol/disulfide exchange in proteins can lead to protein unfolding and loss of the biological function/activity of proteins[39]. Redox active Se compounds do not only affect proteins, but can also cause DNA damage and alter the DNA response through both ROS production and direct interactions or binding[40]. These redox active metabolites are known to cause both single and double strand DNA brakes[41].

The remarkable selectivity for Se accumulation in cancer cells has been known for decades, ever since the use of ^{75}Se-sodium selenite and ^{75}Se-SeMet as scanning agents to diagnose tumours[42]. The selective uptake and accumulation of Se in tumour cells is believed to be a mechanism behind its tumour specific activity. However, the uptake mechanisms are known to vary between Se compounds, even though they are not fully elucidated. It remains a challenge to determine the exact transport mechanism for each Se compound, as they are typically very reactive molecules. The uptake of selenite was shown to be facilitated by the presence of extracellular reducing thiols, suggesting that the reduced form, presumably selenide, was more readily taken up by the cells[43]. More recently, it has been shown that Se accumulation in tumours could be partly explained by the overexpression of the

cystine/glutamate antiporter, xCT, observed in several tumors[44]. This overexpression creates a more reducing extracellular microenvironment, thus facilitating Se uptake by reducing selenite to selenide[45]. Additionally, the selective uptake of Se by cancer cells has also been attributed to their aberrant metabolism, which requires an increased amount of Se, the proposed rate limiting factor for the synthesis of key antioxidant selenoenzymes, such as glutathione peroxidase and thioredoxin reductase[46].

1.5 Natural Organic and Inorganic Selenium Compounds in Cancer Therapy

Selenite

To date, both organic and inorganic Se compounds have been explored in cell and animal cancer models. Selenite has been shown to display cytotoxic effects in the low µM range across a variety of cancer cells, including lung[47,48], prostate[49], cervical[50], ovarian[51], colon[52,53], primary acute myeloid leukemia[54], lymphoblastic leukemia[55], liver[56] and melanoma[57]. It is thought that selenite induces apoptosis by the ROS-mediated mitochondrial pathway [49,50], while there is also evidence supporting the involvement of Bax[53,55,58] and p53[52] in determining the mechanism of cell death. Selenite has also been shown to sensitise cells to a range of classic chemotherapeutic drugs[58–60] and, interestingly, has proven more effective in multi-drug resistant cells[51,61]. Although *in vivo* studies have generally confirmed the anti-tumour potential of selenite, its use as a therapeutic drug is considered to be limited because of its systemic and organ toxicity[13].

Selenodiglutathione (SDG)

SDG is the primary metabolite of selenite but its therapeutic potential has been investigated to a far lesser extent. Across a range of cancer cells, it has been reported that SDG is either equally or more cytotoxic than selenite [40,62–64]. Some studies have accounted for the higher cytotoxicity of SDG through higher intracellular Se accumulation following SDG treatment compared to selenite treatment[62,64] and many studies have suggested that, similarly to selenite, SDG induces apoptosis through ROS-mediated effects, including DNA damage[62–66]. Hence, it has been proposed that due to its similar metabolic pathway and mechanism of action to selenite, SDG also has a limited therapeutic potential. On the contrary, it has also

been reported that selenite can induce a necroptosis-like cell death, whereas SDG can modify proteins through glutathionylation, inducing an apoptosis-like cell death[40].

Selenomethionine (SeMet)

The amino acid SeMet has displayed cytotoxicity toward several cancer cells, including lung, breast, colorectal, prostate and melanoma, among others[67–70]. Although cytotoxicity in cancer cells has typically been observed in the 10^1-10^2 µM range, a strong selectivity toward cancer cells over normal cells has also been observed[67]. More recently, the low systemic toxicity and high tumour selectivity were also observed in an animal model[71]. While there is still debate about what the mechanisms of action are, SeMet treatment has been shown to involve p53 mediated apoptotic cell death[69–71], endoplasmic reticulum stress[69], and cyclooxygenase-2 mediated mechanisms[68].

Selenocysteine/Selenocystine/Seleno-DL-Cystine

Selenocystine (SeC) is a diselenide oxidation product of the amino acid Sec. The cytotoxicity of SeC has been determined in the low µM range in lung, breast and liver cancer cells, as well as in melanoma cells[72–75]. It has been shown that SeC acts through elevating ROS levels and inducing mitochondrial-mediated apoptosis[73–75]. Further, it has been shown that knockdown of TrxR sensitizes cancer cells to the effects of SeC[72] and that SeC enhances the potency of auranofin, an established TrxR inhibitor, lung and breast cancer cells[76,77]. Importantly, Sec has also been shown reduce tumour growth *in vivo* by the induction of apoptosis[74]. However, despite its promise as a cancer therapy agent, the poor stability and solubility of SeC have brought into question its potential for further development.

Methylseleninic Acid (MSA)

The therapeutic potential of MSA has been investigated both in cells and in animal models. The cytotoxicity of MSA toward cancer cells has proven to be highly dependent on the model, ranging from the low- or sub-micromolar level to >10µM in prostate and lung cancer cells[78–81]. Importantly, MSA has been shown to possess selective toxicity to lung cancer cells over normal lung epithelial cells[81]. The mechanism of action of MSA, however, is still an area of debate. In prostate cancer cells, MSA induced a caspase-dependent, mitochondrial-mediated form of apoptosis that requires cell detachment from the extracellular matrix (termed anoikis) but does not require ROS generation[78,79,82]. Moreover, MSA was shown to

induce apoptosis in lung cancer cells through nuclear translocation of FOXO3a, which ultimately disrupted cellular redox homeostasis by decreasing ROS production and resulted in G1 cell cycle arrest. In non-Hodgkins lymphoma cells, MSA was also shown to induce caspase-dependent apoptosis; however, the pro-apoptotic signals were associated with the unfolded protein response (UPR) caused by endoplasmic reticulum (ER) stress[83]. In contrast, breast cancer cells that were treated with MSA displayed high levels of both superoxide generation and mitochondrial membrane depolarisation[84]. Importantly, in a mouse model of prostate cancer, MSA treatment has exhibited promising results: delaying tumour growth, increasing apoptosis levels, lowering proliferation levels and increasing survival, while also displaying no evidence of systemic toxicity[85].

Seleno-methylselonocysteine (MSC)

Substantial *in vitro* cytotoxicity of MSC to cancer cells has only been achieved at relatively high concentrations (medium to high µM range) compared to other Se compounds across a range of colon cancer cells[86] and breast cancer cells[69]. However, the limited potency of MSC *in vitro* can likely be attributed to insufficient β-lyase activity, which is essential to MSC metabolism and is usually present in tissue. Nevertheless, MSC has been shown to inhibit vascular endothelial growth factor (VEGF) expression *in vitro*[69]. Additionally, it has been shown to act synergistically with a range of classic chemotherapeutic compounds *in vivo* by enhancing drug delivery and vascular maturation, down-regulating upstream tumour survival markers, and, importantly, inhibiting tumour growth[87–89]. Interestingly, *in vivo* models have highlighted a protective role for MSC against organ toxicity that would normally be associated with lethal doses of chemotherapeutic compounds[90].

1.6 Dual-action Se Derivatives of Tyrosine Kinase Inhibitors in Cancer Therapy

Novel Se derivatives of Imatinib, Dasatinib and Sorafenib have been synthesised by the group headed by Dr. Giovanni Marzaro at the University of Padua. These compounds were designed with the intention that they retain their endogenous inhibitory activity toward tyrosine kinases and, additionally, function as pro-oxidants due to the incorporation of a potentially redox active selenium moiety. In this way, the compounds can be considered dual-action, targeting both kinase activity and redox homeostasis.

Protein phosphorylation is a tightly regulated post-translational signalling mechanism that is involved in a variety of cellular processes. Kinases catalyse the addition of a phosphate group to a protein, while phosphatases perform the opposite reaction. Aberrant regulation of kinase signalling is associated with several human cancers and, for this reason, kinases have long been recognised as potential targets for cancer therapy[91]. Small molecule kinase inhibitors prevent ATP binding to the ATP binding pocket with varying degrees of selectivity and specificity for the 518 identified human kinases[91]. Additionally, while some of these molecules target the active conformation, others target the inactive conformation of kinases. The requirement for target specificity of small molecule kinase inhibitors is a subject of much debate. Most cancers are linked to the dysregulation of multiple kinase pathways; hence, broader drug specificity could be useful in targeting several kinases[91]. However, non-selective inhibitors would also be more likely to interfere with regular cellular function, leading to more substantial toxic side-effects[91].

Imatinib

Structural analysis has revealed that imatinib acts by binding near the ATP-binding site of the inactive form of BCR-ABL. In turn, this causes a conformational change to the structure of the ABL active site, thus inhibiting BCR-ABL kinase activity[91]. Indeed, Imatinib was first approved for use as a treatment for chronic myelogenous leukemia (CML), a condition caused by the genetic translocation of the c-abl oncogene to the breakpoint cluster region (bcr) on chromosome 22, resulting in a fusion protein (BCR-ABL) that drives abberant ABL kinase activity[91]. However, Imatinib is also known to inhibits other kinases, including c-KIT and PDGFR, which have subsequently broadened its therapeutic use[91].

Dasatinib

Imatinib resistance in CML patients necessitated the investigation into novel second generation BCR-ABL inhibitors. Dasatinib was designed to inhibit both BCR-ABL and, another tyrosine kinase, SRC. It has been shown to possess a potency in the sub-to-low nm range against common BCR-ABL mutations[92]. However, Dasatinib has also been shown to possess non-selective targeting properties, displaying binding affinities below 100nm for 16% of the 287 tested kinases and, in particular, for 47% of the tested tyrosine kinases[93]. It is still a topic of debate to what extents the enhanced efficacy of Dasatinib in Imatinib-resistant patients is due to (1) its higher biochemical potency, (2) its inhibition of a wider range of

BCR-ABL mutations, (3) its SRC inhibition and/or (4) its inhibition of previously unanticipated target kinases[91].

Sorafenib

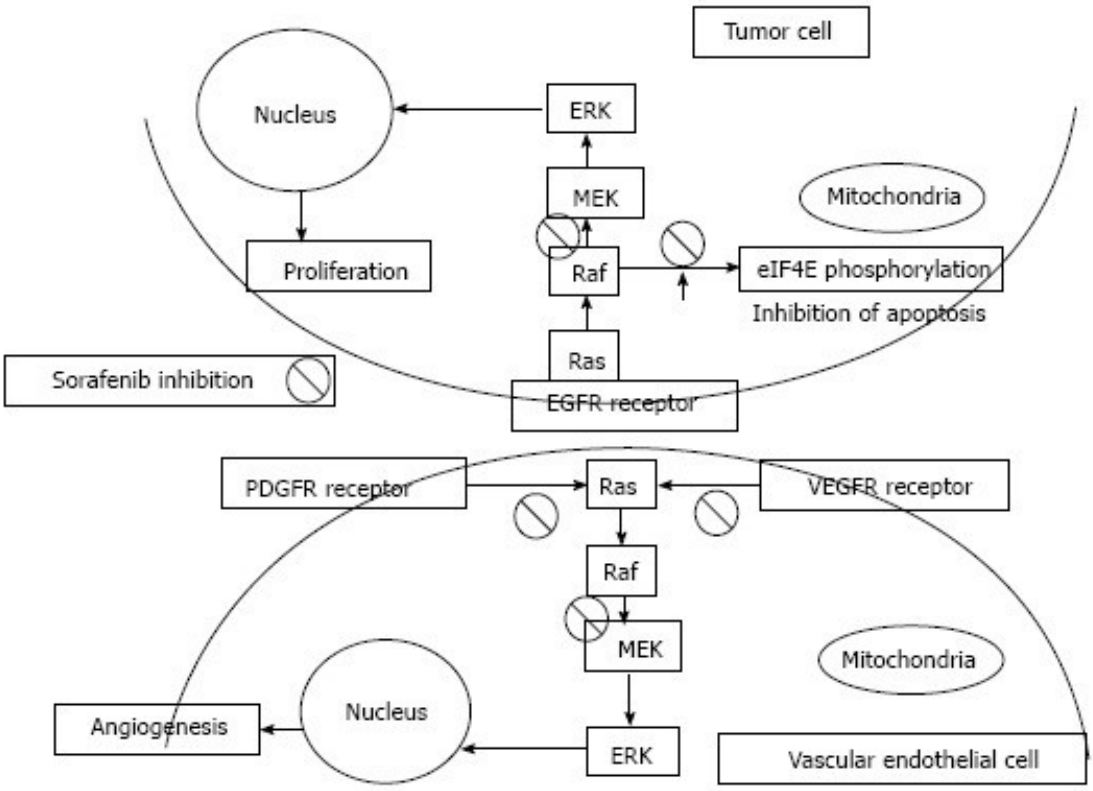

Sorafenib inhibits the Raf/MEK/ERK pathway in both endothelial cells and tumour cells, reducing proliferative signalling and angiogenesis, and blocking the inhibition of apoptosis[94].

Sorafenib is considered a multiple kinase inhibitor, affecting a variety of both intracellular (CRAF and BRAF) and cell surface receptor (several VEGFRs, PDGFR-β, KIT, FLT-3, RET) kinases[91]. Sorafenib acts primarily by inhibiting the Raf/MEK/ERK pathway in both endothelial cells and tumour cells. This ultimately reduces the levels of proliferative and angiogenic signalling, and also blocks the inhibition of apoptosis in tumour cells[94]. Although Sorafenib has been approved for the treatment of advanced renal carcinomas and unresectable hepatocellular carcinomas, it has also been associated with a variety of systemic toxicities. In particular, it is thought that VEGFR inhibition adversely affects cardiovascular and renal homeostasis as well as wound healing and tissue repair[91]. More

recently, a fluorine derivative of Sorafenib, Regorafenib, has received attention in clinical studies, with promising results in patients that had previously received Sorafenib treatment[95].

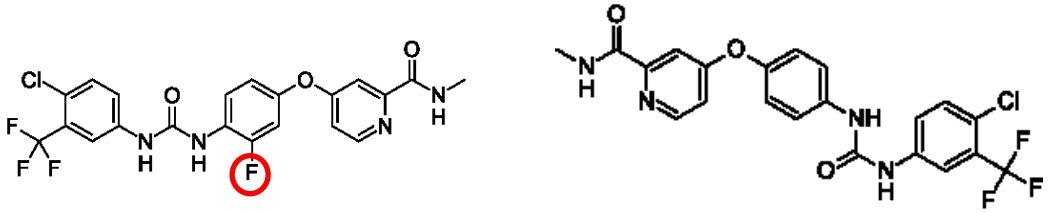

Regorafenib is formed by the addition of fluorine to the central ring of Sorafenib.

1.7 Selenium Compounds as Oxidants in Pancreatic Cancer Therapy

Cancer cells are characterised by an increased production of reactive oxygen species (ROS) and an altered redox environment that facilitates tumour progression and the evasion of ROS-induced cell death[96]. Pancreatic cancer (PC) typically has a poor prognosis associated with a highly aggressive tumour that is operable in only 5-25% of patients, a currently limited chemotherapeutic efficacy and a median survival period of 2-6 or 8-14 months for patients with locally advanced or metastatic disease, respectively[97]. Recently, a key role in carcinogenic processes has been identified for PC-associated K-Ras mutation, which occurs in up to 90% of cases[98]. Although the role of oncogenic K-Ras expression is still under investigation, a high level of sustained K-Ras is required for pancreatic tumorigenesis and ultimately favours enhanced glycolysis and reduced dependence on the Krebs cycle, promoting a reducing environment that facilitates PC cell growth and invasion potential[98]. Specifically, it has been shown that mutant K-Ras transfection can transform immortalised pancreatic duct epithelial cells, inducing increased levels of ROS and higher NADPH oxidase activity and expression[99]. Cancer cells regulate oxidative stress through the induced up-regulation of antioxidant defences; however, this capacity can be considered to be "maximised", leaving them vulnerable to additional oxidative stress[100]. Notably, it has been shown that K-Ras mutated cell lines are more susceptible to an increase in oxidative stress[101]. Hence, targeting the inhibition or consumption of antioxidant pathways in PC cells is a promising, novel therapeutic[13,100].

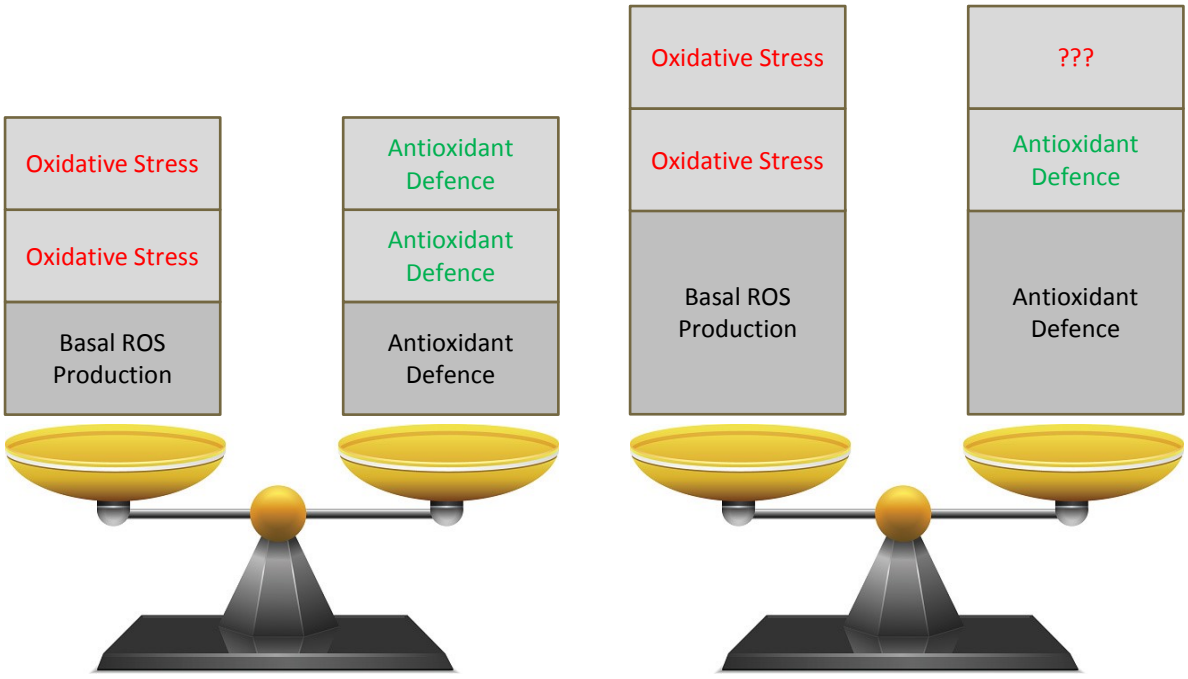

Normal Cells **Tumour Cells**

Tumour cells, in order to tolerate higher basal levels of ROS production, are endowed with a higher basal level of antioxidant defence. However, upon further oxidative stress, cancer cells are thought to have a reduced capacity to up-regulate their antioxidant defence, which is considered to be maximised.

At physiological concentrations, Se is considered to be critical for cellular antioxidant defence because of its classic role in selenoprotein synthesis. More recently, however, the pronounced redox activity of Se has been investigated for its potential as a toxic, growth-inhibiting pro-oxidant in cancer therapy. The cytotoxic effects of Se compounds and their metabolites are dependent upon the generation of free selenols and selenolates through reduction reactions, either chemically by thiols (either free or protein-bound) or enzymatically by reductases. These selenols and selenolates are, in turn, highly reactive and consume both NADPH and thiols, resulting in the generation of oxidative stress[13,102]. Naturally occurring Se compounds, including selenite, Sec, MSA and MSC are all known to possess this cytotoxic potential at supra-nutritional concentrations. Additionally, many novel Se compounds are currently being synthesized and investigated for their potential as pro-oxidant cancer therapeutics.

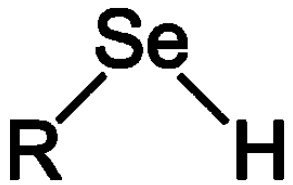

Supranutritional levels of Se leads to the production of selenols and selonolates, which react with oxygen and thiols and induce oxidative stress.

Se derived pro-oxidant therapy necessitates that the cytotoxic effects of compounds are achieved at lower doses in cancer cells than in normal cells, due to the aforementioned shift in cancer cell redox homeostasis. In addition, the specific uptake and accumulation of Se in cancer cells has also been highlighted as a key determinant of its potential as a therapeutic agent[45]. Hence, a therapeutic window exists, within which, the dose of Se is cytotoxic to cancer cells while being sub-toxic to normal cell[13,100]. However, it is not only the concentration of Se compounds that determine their potency. Since the biological activity of Se compounds are largely determined by their metabolites, the chemical structure and the metabolic pathway it engages are critical determinants of the redox potential of compounds and hence their effect in vivo[22,40].

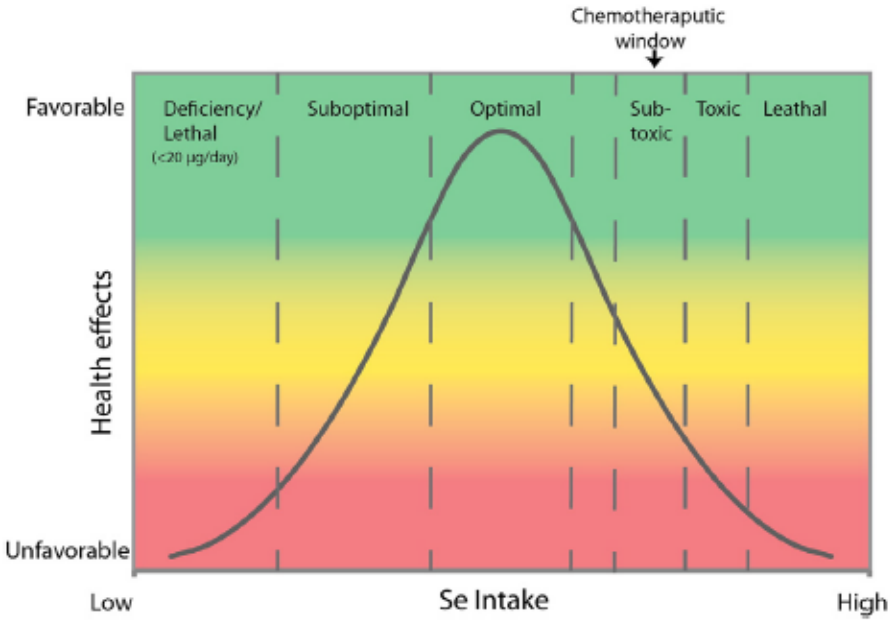

The chemotherapeutic window for redox active Se compounds[13]. Ideally, Se-based chemotherapeutics should be delivered at a dose that is sub-toxic to normal cells that is

also toxic/lethal to tumour cells. In this manner, Se-based chemotherapeutics target the redox "Achilles heel" of tumour cells.

1.8 K-Ras Mutation and Pancreatic Cancer

K-Ras mutation is the most common mutation associated with human cancer, and it is therefore among the most heavily studied oncogenes. Mutant K-Ras is detected in approximately 20-30% of all human tumours and, as previously mentioned, in up to 90% of PC cases[99]. K-Ras is part of the Ras family of small GTPases (which also includes H-Ras and N-Ras) and it is activated by GTP binding to its guanine nucleotide binding site. Wild-type Ras, however, is typically bound to GDP. The loading of GTP in place of GDP is not spontaneous, requiring interaction with activating molecules, such as guanine exchange factors, which are themselves stimulated by extracellular signalling molecules. Additionally, Ras proteins have intrinsic GTPase activity, which, aided by GTPase-activating proteins, hydrolyses GTP to GDP and returns Ras to an inactive state. Therefore, physiological Ras activity is transient and tightly regulated[99]. Importantly, Ras has many downstream effectors and is therefore involved in several cellular processes including: growth, proliferation, survival, inflammation, transformation and senescence[99].

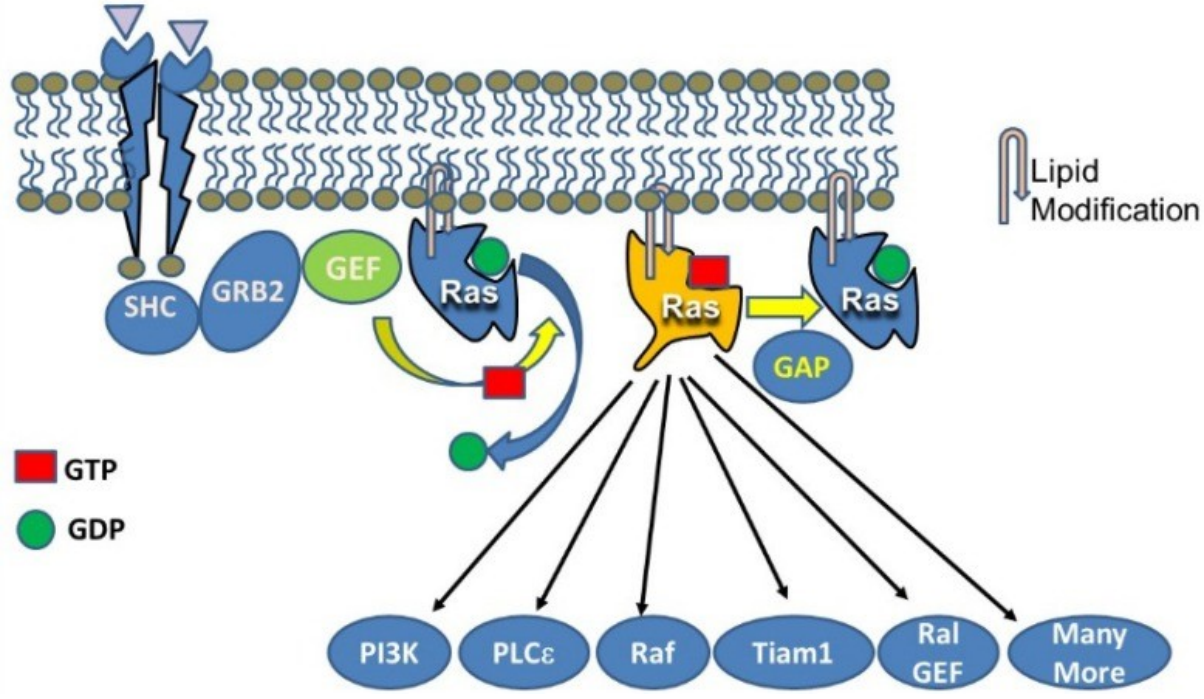

RAS signalling regulates several processes that are involved in cellular transformation[99]. The total cellular RAS activity is higher in cells carrying K-Ras mutation due to reduced activity of GTPase-activating proteins (GAPs), which are responsible for RAS inactivation.

The mutant form of K-Ras that is commonly associated with cancer acquires a point mutation of either residue 12 or 61. These mutations disrupt the interaction between Ras and GTPase-activating proteins, hence lowering the rate of GTP hydrolysis to GDP and increasing Ras signalling. In contrast to the classic model of pancreatic tumorigenesis being driven by constitutive oncogenic K-Ras signalling, it has recently been proposed that there is, instead, prolonged signalling following mutant K-Ras activation. Hence, the presence of mutant K-ras is not sufficient for cellular transformation, but rather, mutant K-Ras enhances the level of Ras signalling in response to stimulants. A high level of Ras activity is necessary for cellular transformation because there is a threshold, above which, Ras activation becomes self-sustaining. Elevated Ras signalling activates several downstream pathways (including ROS signalling, NFκB, Cox2 and Stat3 pathways) that generate Ras activators, giving rise to the "Ras/Inflammation Feed-Forward Model" of PC initiation[99].

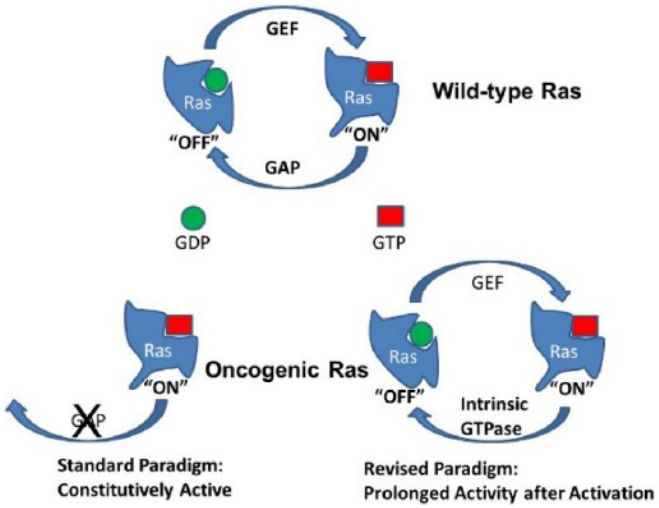

In the revised paradigm of RAS mutation, rather than constitutively active RAS activity there is prolonged RAS activity following RAS activation due to reduced GTPase activity, which is necessary for RAS inactivation[99].

Thesis Aims and Goals

Given the demand for novel therapeutic approaches to the treatment of aggressive, malignant tumours, we investigated the anti-tumour capacity of several Se compounds. Specifically, we investigated the potency of two different classes of Se compounds. For the purposes of this thesis, the studies have been divided into two parts:

(Part 1) Simple organic Se compounds: Seleno-L-cystine (SeC), Methylselenic Acid (MSA) and Se-(Methyl)selenocysteine (MSC). These three compounds occur naturally and are major constituents of dietary Se. They have been extensively studies in recent years as potential chemotherapeutic drugs in a range of common cancers including breast, lung, colorectal, skin (melanoma) and liver. However, there is limited data on the effects of these compounds in pancreatic cancer.

(Part 2) Selenium derivatives of tyrosine kinase inhibitors (TKIs) that were developed as multi-targeting agents, based on the scaffolds of Imatinib (GY811), Dasatinib (GY812) and Sorefenib (GY813). These compounds were synthesized by the Chilin/Marzaro group at The University of Padova.

The primary aims of this thesis are:

(1) To evaluate the cytotoxicity of Se derivatives by performing and comparing the results of multiple cell viability assays, including the MTT, SRB and Neutral Red assays, in human pancreatic cancer cell lines that either express or do not express mutant K-Ras, as well as in non-transformed cells.

(2) To determine the cellular uptake of Se compounds by means of graphite furnace atomic absorption spectroscopy (GF-AAS) and evaluate its correlation with cytotoxicity.

(3) To determine the extent to which Se compounds induce ROS generation and mitochondrial membrane depolarisation in PC cells using fluorescence-based assays.

(4) To examine the effects of Se compounds on antioxidant enzyme activity by extracting cell lysates and performing standard absorbance-based enzyme activity assays.

(5) To examine changes in mRNA expression of several redox genes in PC cells treated with Se compounds using quantitative real-time PCR (qPCR).

(6) To determine the efficacy of lead compounds in an *In Vivo* murine model of cancer (Lewis Lung Carcinoma, LLC) by examining the effects on tumour growth.

(7) To compare the efficacy of TKI Se derivatives in a 3D-spheroid cell culture model using a variety of cell viability analysis techniques.

2 Materials and Methods

2.1 Selenium Compounds

All organic Se compounds (MSA, SeC and MSC) were purchased from Sigma Aldrich. All TKIs and their Se-derivatives were synthesised by the lab group headed by Dr. Giovanni Marzaro in the Department of Pharmaceutical Sciences at the University of Padua. The structure of all compounds are shown below.

2.1.1 Simple Selenium Compounds

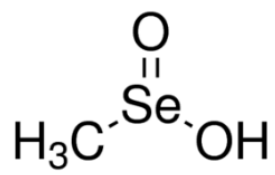

Methylseleninic Acid (MSA)

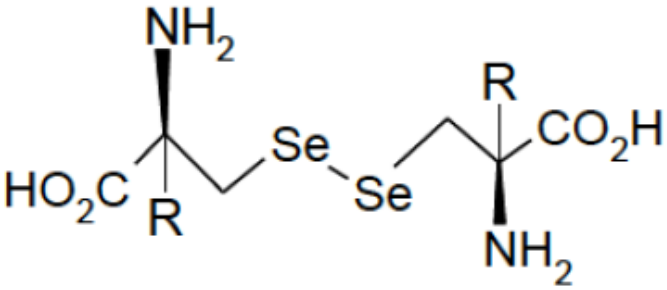

Selenocystine (SeC)

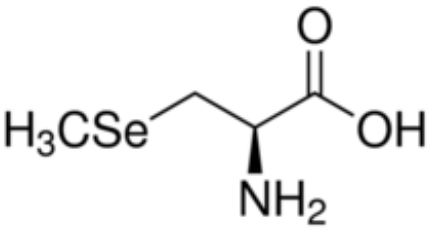

Se-(Methyl)selenocysteine (MSC)

2.1.2 Tyrosine Kinase Inhibitor Selenium Derivatives

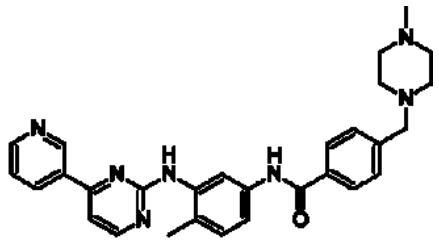

Imatinib

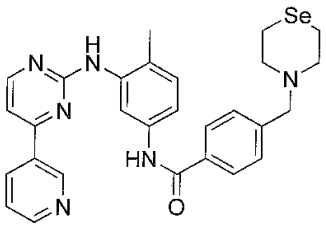

GY811

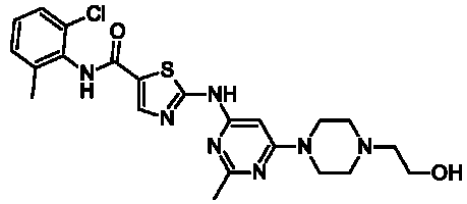

Dasatinib

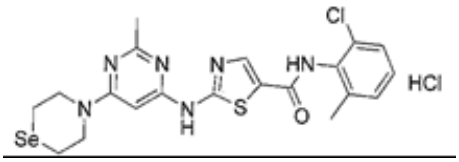

GY812

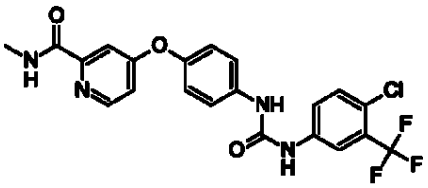

Sorafenib

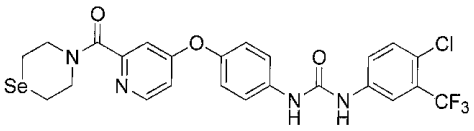

GY813

2.2 Cell Lines and Cell Culturing

All cell lines were cultured and maintained at 37ºC in a humidified atmosphere with constant 5% CO2 in 25cm^2 or 75cm^2 flasks. Cells were grown in DMEM (for PANC1 and HEK293) RPMI (for PNS1 and BxPC3) or MEM (for #18 glioma cells) supplemented with 10% FBS, 2mM glutamine and 1% Penicillin-streptomycin.

The details and origins of the pancreatic cancer cell lines used in the experiments are as follows:

PSN1 (K-Ras mutant)

The PSN1 cell line is derived from human pancreatic adenocarcinoma. PSN1 cells are unique in their K-Ras expression profile. The amplification of mutant K-ras (with a point mutation from GGT to CGT at codon 12) is present at the same level as observed in the primary tumour (3-6 fold), as is the amplification of Myc (50-fold). Additionally, one of the p53 alleles is lost, while the other carries a point mutation (AAG to CAG at codon 132).

PANC1 (K-Ras mutant)

The PANC1 cell line is derived from a pancreatic ductal carcinoma from a 56 year old Caucasian male. The cell line carries both a K-Ras mutation (12 Asp) and P53 mutation (273 His/Cys)

BxPC3 (K-Ras wild-type)

The BxPC3 cell line is derived from a primary pancreatic adenocarcinoma from a 61 year old female. The cell line does not carry a K-Ras mutation but it does possess a P53 mutation (220 Cys).

Glioma #18 Cells

The glioma #18 cells are a highly drug-resistant patient derived cell line, used in collaboration with Dr. Lars Brautigam at Karolinska Institutet.

2.3 Cytotoxicity Assays

Three different types of cell viability assays, the MTT, SRB, and Neutral Red methods, were performed in order to examine the cytotoxicity of Se compounds in cells. Since the three assays measure cell viability based on the functional activity of different sub-cellular components, it was also possible to gain insight into the possible mechanisms of action of the compounds.

The MTT assay relies upon cellular oxidoreductase activity, which, under specific conditions, reflects mitochondrial function and hence cell viability. In this assay, MTT (3-(4,5-Dimethylthiazol-2-yl)-2,5-Diphenyltetrazolium Bromide) is reduced by living cells to an insoluble purple formazan. The formazan must then be dissolved before reading its absorbance.

3-(4,5-dimethylthiazol-2-yl)-2,5-diphenyltetrazolium bromide (MTT)

(*E*,*Z*)-5-(4,5-dimethylthiazol-2-yl)-1,3-diphenylformazan (Formazan)

The SRB assay is dependent upon the staining of fixed protein amino acid residues to measure cell density, which ultimately reflects the level of cell proliferation. In this assay, SRB (sulforhodamine B) dye binds proteins under mildly acidic conditions and can then be extracted under basic conditions to measure the total protein levels.

The Neutral Red assay relies upon the ability of viable cells to uptake a supravital dye into lysozomes, and hence utilises the function of lysozomes and the Golgi apparatus as an indicator of cell viability. As cells begin to dye their capacity to uptake the dye diminishes, and the total amount of dye incorporated into cells can be determined by light absorbance.

Experimental Procedure:

For all methods, cells were seeded at a concentration of 3-5x10^3 cells per well in 96-well plates. After 24 hours, cells were treated for 72 hours at increasing concentrations of Se compounds, ranging from 0.037-243µM. The mean absorbance for each drug dose was expressed as a percentage of the control well absorbance and plotted against drug concentration. IC50 values were determined and represent the drug concentrations that reduce the mean absorbance to 50% of that detected in the control wells.

2.3.1 MTT

After treatment with Se compounds, 10 µL of 5 mg/mL MTT (3-(4,5-dimethylthiazol-2-yl)-2,5-diphenyltetrazolium bromide) saline solution was added to each well and allowed to metabolise during an additional 5 hours of incubation. Then, 100 µL of sodium dodecyl sulfate (SDS) solution in 0.01 M HCl was added to each well in order to solubilise the formazan salt crystals. After overnight incubation with the SDS solution, the inhibition of cell growth induced by the compounds was detected by measuring the absorbance of each well at 570 nm using a Bio-Rad 680 microplate reader.

2.3.2 SRB

After treatment with Se compounds, cells were fixed by adding 25µL of 50% trichloroacetic acid (TCA) to each well (final concentration 10% TCA) and incubated at 4^{o}C for 1 hour. Wells were then rinsed 3 times with 200µL water. 50µL of 0.4% SRB solution was added to each

well and allowed to incubate for 15 minutes at room temperature. Wells were rinsed 5 times with 1% acetic acid solution and then allowed to dry. 100µL of 10mM Tris solution was added to each well in order to resuspend the SRB. The inhibition of cell growth induced by the compounds was detected by measuring the absorbance of each well at 590 nm using a Bio-Rad 680 microplate reader.

2.3.3 Neutral Red

After treatment with Se compounds, cells were incubated in 100µL of filtered neutral red solution (50µg/mL) for 3 hours at 37C^{o}. Subsequently, wells were aspirated and 200µL of a 50% ethanol/1% acetic acid solution was added to each well and left for 20 minutes. The absorbance was measured at 520nm with a Bio-Rad 680 microplate reader.

2.4 Cellular Uptake

The capacity of compounds to accumulate in cells is a key determinant of their efficacy and can be determined by graphite furnace atomic absorption spectroscopy (GFAAS). GFAAS involves the vaporisation of samples in a graphite coated furnace in order to atomise the sample. Free atoms in the sample will absorb UV/visible light resulting in electron transitions into higher energy levels. Importantly, free atoms of a specific element (for this study, selenium) will absorb light at characteristic wavelengths and the absorption of light at this wavelength is linearly proportional to the amount of that element in the sample. By comparing the atomic absorption of Se in cells treated with Se compounds, it is possible to estimate and compare the cellular accumulation of the compounds.

Experimental Procedure:

To examine the correlation between cellular uptake and cytotoxicity, cells were seeded at 7.5x10^{5} cells in 75cm^{2} flasks. After 24 hours, the medium was replaced and the cells were treated with Se compounds for 24hours at a concentration of 2.5µM. Subsequently, cells were washed with PBS, harvested and counted. An aliquot was also used for the determination of protein content with a standard Bradford assay. Samples were stored at -20ºC until further use. Samples were subjected to five 20 minute freeze-thaw cycles at -20

°C and then vortexed. Samples were mineralised in 500µL of highly purified nitric acid (Se: ≤0.005µg/kg) and 500µL hydrogen peroxide. Samples were then transferred into a microwave Teflon vessel before being subjected to the standard procedure using a speed wave MWS-3 Berghof instrument. After cooling, the selenium content of each sample was determined using a Varian AA Duo graphite furnace atomic absorption spectrometer at a wavelength of 196 nm. A calibration curve was obtained using standard solutions of known Se concentrations.

2.5 ROS Production

ROS production is a well-established indicator of oxidative stress in cells. Chemically reduced and acetylated forms of 2',7'-dichlorofluorescein (DCF) are non-fluorescent. However, once the acetate groups are removed by intracellular esterase activity, oxidation of the molecule can occur, resulting in a fluorescent product. CM-H2-DCFDA (5-[and -6]-chloromethyl-2',7'-dichlorodihydrofluorescein diacetate) is therefore a useful indicator of cellular ROS levels, with the added advantages of passively diffusing into cells and a high retention level.

Experimental Procedure:

To examine ROS generation, cells were seeded in 96 well plates at 10^4 cells per well in phenol red-free RPMI. After 24 hours, cells were washed with PBS/10mM glucose and then loaded with 10µM CM-H2-DCFDA in the same buffer for 20 minutes in the dark. Cells were washed again with PBS/10mM glucose and incubated with either 5 or 50µM Se compounds in the phenol red-free medium. Antimycin (3µM), a potent inhibitor of Complex III in the electron transport chain, was used as a positive control. The increase in fluorescence of DCFDA over time was measured using an excitation wavelength of 485 nm and an emission wavelength of 527 nm in a Fluoroskan Ascent FL plate reader.

2.6 Mitochondrial Membrane Potential

Mitochondrial ROS production plays an important physiological role in cell signalling. However, at high levels, ROS-induced mitochondrial damage results in depolarisation of the

mitochondrial membrane and, typically, also in apoptotic cell death. The membrane-permeable JC-1 dye can be used to monitor mitochondrial health. JC-1 accumulates in the mitochondria in a potential-dependent manner, reflected by a fluorescence emission shift from green (529nm) to red (590nm). Hence, a decrease in the red/green fluorescence intensity ratio can be observed in cells exhibiting depolarised mitochondrial membranes. The potential-dependent shift is a result of the formation of red fluorescent J-aggregates.

Experimental Procedure:

To examine mitochondrial membrane depolarisation, cells were seeded at 10^4 cells per well in 96 well plates. After 24 hours, cells were treated with Se compounds at a concentration of 5 or 50µM. Antimycin (3µM), a potent inhibitor of Complex III in the electron transport chain, was used as a positive control. Cells were then loaded with JC-1 (10µg/mL) dye according to the manufacturer's instructions. Fluorescence was measured using an excitation wavelength of 490nm and an emission wavelength of 590nm in a Fluoroskan Ascent FL plate reader.

2.7 Antioxidant Enzyme Activity

To maintain redox homeostasis under conditions of oxidative stress cells must up-regulate their antioxidant defences. One of the ways this can be achieved is through increasing reductive enzyme expression/activity. The capacity to tolerate oxidative stress is considered to be a potential pathway in which various cancer cells as well as non-transformed cells differ metabolically.

Experimental Procedure:

For all enzyme activity assays, cells were treated with 2.5µM Se compound in fresh medium for 24 hours. Cells were then harvested and rinsed in PBS to remove residual medium. 500µL of RIPA buffer was added to cell pellets and the samples were left on ice for 5 minutes before being vortexed. To extract the protein lysate, samples were centrifuged at 10000g for 8 minutes and the supernatant was collected and stored on ice for immediate use. To determine protein concentration, a standard (Bio Rad) protein quantification assay

was performed. For the TrxR and GR assays, 50ng total protein was used for each sample, while for the GPx assay, 200ng total protein was used for each sample.

2.7.1 Thioredoxin Reductase

Thioredoxin reductase (TrxR) activity can be measured in cell lysates by examining the enzymatic reduction of DTNB (5,5'-Dithiobis(2-nitrobenzoic) acid) in the presence of NADPH. This reaction results in the production of TNB (5-thio-2-nitrobenzoic acid), whose absorbance can be determined at 412nm. The *in vivo* reduction reaction (with thioredoxin (Trx) as a substrate) and the experimental reaction are as follows:

(TrxR *In Vivo*)

$$TRX\text{-}S\text{-}S + NADPH + H^+ \leftrightarrow TRX\text{-}(SH)2 + NADP^+$$

(TrxR Assay)

$$DTNB + NADPH + H^+ \leftrightarrow 2\ TNB + NADP^+$$

Experimental Procedure:

The final reagent concentrations were 50ng total protein (from sample) and 0.2mM NADPH in 0.1M phosphate buffer (pH 7.4). To start the reaction, DTNB was added at a final concentration of 0.06mM. After 15 minutes, the absorbance at 412nm was measured in a 96-well plate using a Bio Rad 680 Plate Reader. The average absorbance in treated samples relative to untreated controls was used to determine relative TrxR activity.

2.7.2 Glutathione Reductase

Glutathione reductase (GR) activity can be measured in cell lysates by examining the reduction of oxidised glutathione (GSSG) to reduced glutathione (GSH). GSH production is coupled to the reduction of DTNB, resulting in the formation of TNB, whose absorbance can be determined at 412nm. The experimental reactions are as follows:

(GR)

$$NADPH + H^+ + GSSG \rightarrow NADP + 2\ GSH$$

Followed by

$$GSH + DTNB \rightarrow GS\text{-}TNB + TNB$$

Experimental Procedure:

The final reagent concentrations were 50ng total protein (from sample), 1mM GSSG, and 0.75mM DTNB in 0.1M phosphate buffer (pH 7.4). To start the reaction, NADPH was added at a final concentration of 0.1mM. After 15 minutes, the absorbance at 412nm was read in a 96-well plate using a Bio Rad 680 Plate Reader. The average absorbance in treated samples relative to untreated controls was used to determine relative GR activity.

2.7.3 Glutathione Peroxidase

Glutathione peroxidase activity can be determined indirectly in cell lysates. In this technique, the oxidation of GSH to GSSG is catalyzed by GPx in the presence of an organic peroxide R-OOH. This is then coupled to the recycling of GSSG back to GSH by GR and NADPH. The decrease in NADPH can be measured at 340nm and reflects GPx activity, since GPx is the rate limiting factor in the coupled reactions. The experimental reactions are as follows:

(GPx)

$$R\text{-}OOH + 2\ GSH \rightarrow R\text{-}OH + GSSG + H2O$$

(GR)

$$GSSG + NADPH + H^{+} \rightarrow 2\ GSH + NADP^{+}$$

Experimental Procedure:

The final reagent concentrations were 200ng total protein (from sample), 0.25U mammalian GR, 2mM reduced glutathione, and 0.1mM NADPH in Tris-HCl buffer (50mM Tris-HCl, 0.2mM EDTA, pH 7.8). To start the reaction, ter-Butyl hydroperoxide was added at a final concentration of 30µM. The absorbance at 340nm was read for 5 minutes, every 30 seconds with a UV spectrophotometer. To determine relative GPx activity, the rate of change in absorbance was determined for each sample and then expressed relative to the control reaction (also accounting for the spontaneous decay of NADPH).

2.8 Antioxidant Gene Expression by RT-qPCR

Real-time reverse transcription quantitative polymerase chain reaction (RT-qPCR) is a method used to examine gene expression by quantifying RNA levels from a biological sample. In RT-qPCR, a fluorescent probe or dye is incorporated into double-stranded DNA molecules that are generated throughout the course of the reaction. Importantly, the amount of product formed during the reaction is progressively monitored by reading the fluorescent signal at the end of each reaction cycle. The number of amplification cycles required to obtain a threshold fluorescent signal (i.e. amount of DNA) can be determined for specific genes of interest and compared across samples. Housekeeping gene expression is also determined in order to normalise the expression of target genes across samples.

Experimental Procedure:

PSN1 and BxPC3 cells (2-3x10^5) were seeded in 25 cm^2 flasks. After 48 hours, the medium was replaced with fresh medium containing 2.5-5 µM dissolved Se compounds. After 24 hours of incubation, cells were washed in PBS and pellets were harvested for immediate use. Extraction of total RNA was performed using the Qiagen (Hilden, Germany) RNeasy Plus Mini Kit, including the optional DNase digestion column, according to manufacturer's instructions. RNA was quantified using a Nanodrop® Spectrophotometer ND-1000 (Thermo Fisher Scientific, Wilmington, DE, USA). cDNA Synthesis was performed using the Maxima First Strand cDNA synthesis kit (Thermo Fisher Scientific), with 1 µg total RNA, according to manufacturer's instructions. Real-time qPCR with 0.25 ng cDNA per reaction was performed in a PikoReal™ Real-Time PCR System (Thermo Fisher Scientific) using Luminaris Color HiGreen qPCR Master Mix (Thermo Fisher Scientific) according to the manufacturer's instructions. mRNA transcript levels were determined for thioredoxin reductase 1(TXNRD1), heme oxygenase 1 (HMOX1) and glutamate-cysteine ligase modifier subunit (GCLM), and their expression was analysed using the standard comparative CT method with actin as a housekeeping gene.

2.9 Thiol Determination Assay

Thiols are extremely efficient antioxidants that play a critical role in protecting cells from peroxidative damage. The availability of free thiols in the cellular environment reflects the

cellular redox state because, typically, under conditions of oxidative stress, free sulfhydryl groups are consumed and, thus, disulfide levels increase. The most common free sulfhydryl groups found in cells include GSH, free cysteine, and cysteine residues on proteins. The level of total free thiols can be determined by their reaction with DTNB, resulting in the formation of 5-thionitrobenzoic acid and a mixed disulphide. The absorbance of the product can be read at 412nm.

Experimental Procedure:

To determine and compare the availability of free thiols, cells ($7.5x10^5$) were seeded in $75cm^2$ flasks. After 24 hours, the medium was replaced and the cells were treated with Se compounds at a concentration of 2.5µM for 24hours. Cells were then harvested and rinsed in PBS. An aliquot was used for the determination of protein content with a standard Bradford assay. Cell pellets were resuspended in 950 µL TE buffer with 7M guanidine hydrochloride. To start the reaction, 30 µL DTNB (3mM) was added to each sample. After 10 minutes, the absorbance was read at 412 nm in a 96-well plate using a Bio Rad 680 Plate Reader. The absorbance values were first normalised to total protein content and then the total free thiol levels were compared to those of the untreated controls.

2.10 Transmission Electron Microscopy

Transmission electron microscopy (TEM) is a high-resolution imaging technique that can be used to examine cellular ultrastructure. In particular, the integrity of nuclei, mitochondria as well the golgi apparatus and lysosomes can be observed.

Experimental Procedure:

Changes in the ultrastructure of PSN1 and BxPC3 cells after 24 hour treatment with Se compounds were examined by TEM according to standard protocols. Briefly, after treatment, cells were collected by centrifugation, washed twice with PBS, and then fixed in Karnovsky solution (2% paraformaldehyde/2.5% glutaraldehyde in 0.1 M sodium cacodylate/HCl buffer, pH 7.4). Postfixation was performed in 1% osmium tetroxide /1.5% potassium ferrocyanide, followed by dehydration and drying. Samples were then trimmed,

mounted and coated, and the ultrathin sections were observed and imaged by TEM (Hitachi JEOL H-7650).

2.11 In Vitro DNA Interaction Assays

2.11.1 Calf Thymus(CT)-DNA Binding Assay

The absorbance spectrum of DNA in physiological solution is well defined. By examining the absorbance spectra of DNA following incubation with increasing concentrations of other compounds, their capacity to intercalate with DNA can be determined. Intercalation is typically associated with an absorbance shift relative to the absorbance spectrum of untreated DNA.

Experimental Procedure:

CT-DNA was rehydrated overnight in 0.1 M phosphate buffer (pH 7.4) at a concentration of 1 mg/mL. Se compounds were incubated with 30 µM CT-DNA in Tris buffer (pH 7.4) at a molar ratio 1:1, 0.7:1 or 0.5:1 (compound:CT-DNA) for 1 hour at 37^{o}C. The absorbance spectrum (from 230 to 500 nm) was determined for each treatment condition using a computer-controlled Varian Coulter DU 800 spectrophotometer and compared to that of the untreated control.

2.11.2 pUC19 DNA Cleavage Assay

pUC19 is a 2686 base-pair double stranded DNA plasmid vector. Greater than 90% of plasmids are in the supercoiled form under physiological conditions. Incubation with agents that directly damage or cut DNA can alter the supercoiled structure of pUC19, which can be detected by gel electrophoresis. Typically, plasmids can be viewed on gels in three different forms: supercoiled, open circular or linear. If the DNA is completely digested, DNA fragments may not be detected on the gel.

Experimental Procedure:

Plasmid pUC19 DNA (2686bp) (500ng per reaction) was incubated with 50 µM Se compounds for 6 hours at 37^{o}C in Tris-NaCl buffer (pH 7.2). After incubation, the samples were mixed with 6x loading dye and loaded onto a 1.5% agarose gel in TAE buffer. Gel electrophoresis was performed at 75V for 2 hours. The gel was left over night in TAE buffer containing 0.5 µg/ml EtBr. The gel was rinsed in TAE buffer and then imaged under UV transillumination (UVP Inc., Upland CA) using an Olympus Camelia C-4040 digital camera (Olympus).

2.12 In Vivo Mouse Lewis Lung Carcinoma (LLC) Model

Animal models provide a means to examine both the efficacy of lead anti-tumour compounds and, simultaneously, monitor their non-specific and systemic toxicities in a living organism. The LLC model is a widely-used, standard mouse model that involves transplantation of cultured tumour cells into mice.

Experimental Procedure:

All experiments were performed according to D.L.G.S. 26/2014, which oversees the care of animals used in experiments in Italy. The research project was approved by the Italian Health Department according to article 7 of above mentioned D.L.G.S. The LLC cell line was purchased from ECACC. Cells were maintained in DMEM supplemented with 10% heat-inactivated FBS (Euroclone), 10 mM l-glutamine, 100 U/mL penicillin, and 100 µg/mL streptomycin in 5% CO2 at 37 °C. The LLC was implanted intramuscularly as a 2x10^{6} cell inoculum into the right hind leg of 8-week old male and female C57BL mice (24 ± 3 g body weight). 24 hours after tumour implantation, mice were randomly divided into two groups (8 animals per group, 10 controls). From day 7 after tumour inoculation (visible tumour), animals were treated daily with a single intra-peritoneal dose (3 mg/kg) of MSA, selenite or Cisplatin (CDDP) dissolved in 0.9% saline. At day 15, animals were sacrificed, the legs were amputated at the proximal end of the femur, and the inhibition of tumour growth was determined according to the difference in weight of the tumour-bearing leg and the healthy leg, expressed as a percentage of the untreated control animals. Body weight was measured at day 1 and every two days from day 7. Body weight changes were considered as a

parameter for systemic toxicity. Data represents the means ± S.D. of at least three separate animal cohorts.

2.13 Cytotoxicity Assays in Resistant Glioma (#18 Cells) 3D spheroids

To further examine the antitumor potential of GY813, a series of cell viability assays were performed in a 3D spheroid cell culture model of resistant glioma (#18) cells. In 3D models, proliferating, non-proliferating and necrotic cells typically remain together, creating a more heterogenic cellular environment that better reflects the in vivo tumour. Additionally, in 3D models, drug efficacy is also determined by its ability to penetrate the spheroid, providing a more realistic situation than 2D models, where compounds are delivered to all cells without penetrating through the tumour mass. To evaluate cell viability after drug treatment under both normoxic and hypoxic conditions, several markers were used: (1) Hoechst staining: a cell-permeable dye that binds DNA; (2) Propidium Iodide (PI) Staining: a nucleic acid dye that cannot cross the membrane of living cells but rapidly penetrates dead/dying cell membranes; (3) Lysotracker® staining: a fluorescent, acidotropic probe for labeling acidic organelles in live cells; (4) LOX-1 staining: a hypoxia sensitive fluorescent probe; and (5) CellTiter-Glo®: a luminescent probe for the quantification of ATP in living cells.

Experimental Procedures:

Spheroid Imaging: Cells were seeded at 2 x 103 cell per well in GravityTRAP™ ULA 96-well plates (PerkinElmer) in 70 µL of specifically formulated culture media: DMEM/F12 (50%), Neurobasal (50%), B27 supplement (1x), N2 supplement (1x), bFGF (10 ng/mL), EGD (20 ng/mL) and Penicillin/Streptomycin. Spheroids were allowed to grow for 96 hours prior to treatment. The medium was removed according to the specific guidelines for GravityTRAP™ plates and replaced with 70 µL of fresh medium containing dissolved GY813 or Sorafenib at final concentrations ranging from 7.5 – 60 µM. The treatment was performed for 72 hours under either normoxic (37 ^{o}C, atmospheric O2, 5% CO2, humidified) or hypoxic (37 ^{o}C, 1% O2, 5% CO2, humidified) conditions. Wells were then subjected to one of several staining protocols, which required the addition of 10 µL of fresh medium containing dissolved staining solutions. The final staining conditions were (1) Hoechst 33258 (3 µM) and propidium iodide (PI) (2 µM) for 2 hours, followed by removal of medium and fixation in

paraformaldehyde (4%) in PBS; (2) Lysotracker® (100 nM) for 2 hours followed by removal of medium and addition of fresh medium; or (3) LOX-1 (2 μM) for 12 hours (overnight). Spheroids were imaged on an Operetta® High Content Imaging System (PerkinElmer).

CellTiter-Glo® Viability Assay: Cells were seeded and treated as above with minor modifications: (1) cells were seeded and treated in 100 μL of medium in round-bottom 96-well Nunc™ microplates and (2) the medium consisted of phenol red-free RPMI media with bFGF 10 ng/mL and EGF 20 ng/mL. The cell viability assay was performed according to manufacturer's instructions and the wells were luminescence (ATP) was measured using a PerkinElmer EnSpire™ 200 plate reader.

3 Results and Discussion (Part 1): Simple Organic Se Compounds

Given the need for more effective treatments for pancreatic cancer (PC), the first part of this thesis focuses on the assessment of the simple organic Se compounds, methylselininic acid (MSA), selenocystine (SeC) and Se-methylselenocysteine (MSC), as potential anti-tumour agents. While these compounds have been previously studied in other types of cancer, there is limited knowledge about their effects on PC models. As redox active organic Se molecules, these compounds are considered to act as oxidants inside the cell that drive oxidative stress. These compounds may be particularly effective in K-Ras mutated PC cells, since K-Ras mutated cells are known to be susceptible to treatment with oxidants. Moreover, since K-Ras mutation is extremely common in PC tumours, this is of particular clinical relevance. The findings of this study will help pave the way for the future use of organic Se compounds in the treatment of PC.

3.1 Cell Viability Assays

The cytotoxicity of Se compounds was assessed by three different cell viability assays, the MTT, Neutral Red and SRB assays, in order to determine the potency of compounds by evaluating their effects on different subcellular organelles/systems.

For all organic Se compounds, lower IC_{50} values (µM) were determined by the MTT method for the K-Ras mutated PSN1 and PANC1 cells than for the K-Ras wild-type BxPC3 cells. MSA displayed the highest cytotoxicity, with the IC_{50} values of 0.65 ± 0.38, 7.11 ± 0.10 and 14.65 ± 2.58 for PSN1, PANC1 and BxPC3 cells, respectively. For selenite treatment, the IC_{50} values were 12.36 ± 4.53, 5.65 ± 0.98, 16.58 ± 2.60 for PSN1, PANC1 and BxPC3 cells, respectively. Sec was less potent than MSA, with IC_{50} values of 1.78 ± 0.86 and 18.27 ± 2.78 for PSN1 and BxPC3 cells, respectively, while MSC was the least potent compound with an IC_{50} of 12.45 ± 2.95 in PSN1 cells and a very limited cytotoxicity in BxPC3 cells up to 50µM.

Following treatment with MSA, higher levels of cytotoxicity were determined for the K-Ras mutated PSN1 and PANC1 cells than for the K-Ras wild-type BxPC3 cells, with IC_{50} values of 6.17 ± 0.46, 13.73 ± 3.61 and 20.56 ± 7.60, respectively. In comparison, selenite had a comparable effect on all cell lines, with IC_{50} values of 6.16±1.38, 5.09±0.78 and 3.65±1.14 for PSN1, PANC1 and BxPC3, respectively.

For all organic Se compounds, the IC_{50} values (μM) determined by the SRB method were comparable across PC cell lines, regardless of their K-Ras genotype. MSA was determined to be the most potent compound with IC_{50} values of 1.39 ± 0.28 and 1.17 ± 0.44 in PSN1 and BxPC3 cells, respectively. The IC_{50} values (μM) for selenite were 6.64 ± 0.69 and 7.36 ± 1.64, and the IC_{50} values (μM) for Sec were 10.85 ± 1.32 and 8.58 ± 4.08, in PSN1 and BxPC3 cells, respectively. MSC displayed limited cytotoxicity up to a concentration of 27μM.

The relative cytotoxicity of organic Se compounds across PC cell lines varied depending upon the cell viability assay that was used. Specifically, K-Ras mutated PSN1 and PANC1 cells were more sensitive to organic Se compounds than the K-Ras wild-type BxPC3 cells when viability was determined by functional assays, such as the MTT (mitochondrial reductive enzyme function) and the NR (lysosomal function) methods. However, all cell lines were equally sensitive to organic Se compounds when measured by the SRB method, which stains protein non-specifically. This would suggest that in spite of comparable cell densities following organic Se compound treatment, the functional activity of intracellular organelles, such as the mitochondria and lysosomes, is notably lower in K-Ras mutated cells than in K-Ras wild-type cells.

Of the organic Se compounds tested, MSA was the most potent across cell lines. Interestingly, in both the MTT and NR assays, the mean IC_{50} values for MSA treatment were lowest in PSN1 cells, followed by PANC1 and then BxPC3 cells, while in the SRB assay PSN1 and BxPC3 cells displayed similar mean IC_{50} values for MSA treatment. Moreover, it is noteworthy that the effects of the organic Se compound, selenite, and MSA were comparable in BxPC3 cells in the MTT assay, whereas PSN1 cells displayed a selective susceptibility (>10 times) to MSA over selenite. In an analogous manner for the NR assay, PSN1 cells were equally sensitive to MSA and selenite, while BxPC3 were substantially more resistant (>5 times) to MSA than selenite. Importantly, while the IC_{50} values for selenite treatment were comparable across cell lines in all of the cell viability assays, the IC_{50} values for MSA treatment varied significantly across cell lines. Taken together, these findings ultimately support the idea that MSA has the potential to selectively target different types of pancreatic cancer cells, whereas selenite appears to have a more general toxicity toward pancreatic cancer cells. Indeed, one of the major limitations for the therapeutic use of selenite is its systemic toxicity.

MSC displayed very low levels of cytotoxicity across cell lines regardless of which method was used to assess cell viability. The limited efficacy of MSC *in vitro* has been previously observed and is likely attributed to insufficient β-lyase activity in cell culture experiments. However, in vivo, MSC has been shown to possess a similar anti-tumour efficacy to MSA. In in vivo models, β-lyase activity is not a limiting factor and MSC can be readily converted into biologically available methylselenol[103]. Hence, while MSC is not particularly useful in cell culture models, it may continue to display comparable effects to MSA in animal models.

As expected from reports in other cancer cell lines, SeC displayed significant cytotoxicity toward pancreatic cancer cells. Similarly to MSA, SeC was selectively more cytotoxic toward PSN1 cells than BxPC3 cells in the MTT assay, while it had comparable effects on different cell lines in the SRB assay. In general, SeC had a similar cytotoxicity profile to selenite, but was ultimately less potent than MSA across cell types and viability assays. Despite its selective cytotoxicity, SeC is generally considered to be a poor candidate for further development as chemotherapeutic drug due to its poor stability and solubility.

MTT IC50 (µM ± S.E.)			
Compound	**BxPC3**	**PSN1**	**PANC1**
MSA	14.65±2.58	0.65±0.38	7.11±0.19
SeC	18.27±2.78	1.78±0.86	
MSC	>50	12.45±2.95	
Sel	16.58±2.60	12.36±4.53	5.65±0.98

SRB IC50 (µM ± S.E.)		
Compound	**BxPC3**	**PSN1**
MSA	1.17±0.22	1,39±0.28
SeC	8.58±4.08	10.85±1.32
MSC	>27	>27
Sel	7.36±1.64	6.64±0.69

Neutral Red IC50 (µM ± S.E.)			
Compound	**BxPC3**	**PSN1**	**PANC1**
MSA	20.56±7.60	6.17±0.46	13.72±3.61
Sel	3.65±1.14	6.16±1.38	5.09±0.78

Table 1. IC_{50} values for PSN1, BxPC3 and PANC1 cells treated with the organic Se compounds MSA, SeC and MSC. Cells were treated for 72 hours with increasing concentrations of Se compounds. Cytotoxicity was assessed by the MTT, NR and SRB methods and IC_{50} values were calculated by a four parameter logistic model. Data represents the means ± standard error ($P < 0.05$).

3.2 Cellular Uptake

With the aim of determining the correlation between cytotoxicity and cellular uptake, we quantified the accumulation of Se compounds in PSN1 and BxPC3 cells treated for 24 hours with equimolar (2.5 µM) concentrations by GF-AAS. For all organic Se compounds, cellular uptake was significantly higher in PSN1 than in BxPC3 cells. Notably, Se accumulation in PSN1 cells treated with MSA was approximately 10 times higher than that observed in BxPC3 cells. Similarly, Se accumulation was approximately 5 times and 2 times higher in PSN1 cells than in BxPC3 cells treated with Sec and MSC, respectively. Additionally, in PSN1 cells, the cellular accumulation of Se positively correlated with the relative cytotoxicity of the compounds determined by functional cell viability assays. MSA treated cells displayed the highest level of Se accumulation, followed by Sec and then MSC. It is also interesting to note that Se accumulation after treatment with selenite was similar across cell lines, which correlates with the similar level of cytotoxicity observed in PSN1 and BxPC3 cells following selenite treatment.

The cellular uptake of Se compounds correlated positively with their respective cytotoxicity in functional cell viability assays (MTT and NR methods), whereby all organic Se compounds displayed higher levels of Se accumulation in PSN1 cells compared to BxPC3 cells, with the greatest difference being observed for MSA treatments, followed by SeC treatments, and then MSC treatments. This finding suggests that the variation in the potency of organic Se compounds across cell lines is, at least, partly explained by their level of cellular uptake. This may be related to both the transport of Se compounds into cells, which is an essential factor for selenite toxicity45, and the metabolism of Se compounds once inside cells.

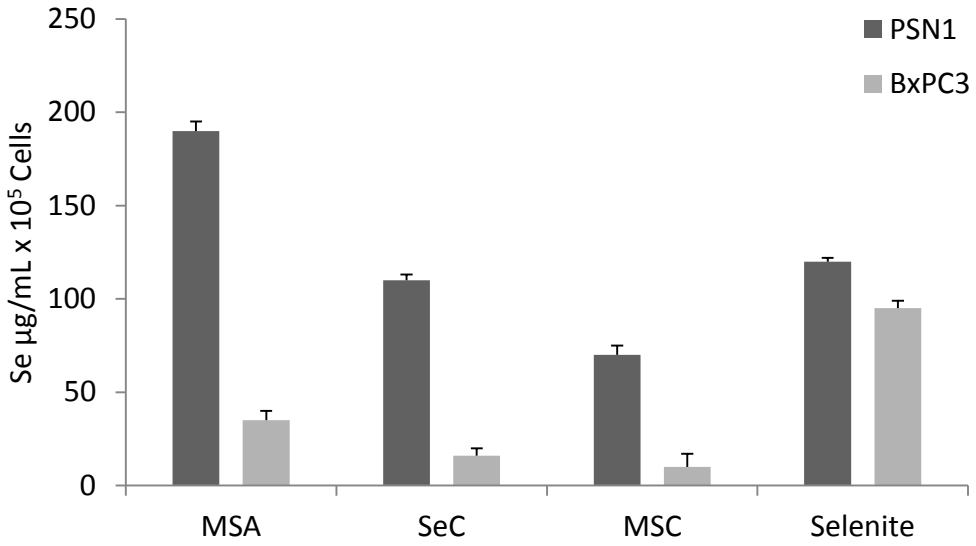

Intracellular accumulation of Se compounds in PSN1 and BxPC3 cells. Cells were incubated with 2.5 µM of Se compounds for 24 hours. The cellular Se content was determined by means of GF-AAS analysis. Data represents the means ± S.D.

3.3 Mitochondrial Effects

Since Se compounds are well known to be redox active, we assessed their mitochondrial effects by assessing ROS production and mitochondrial membrane depolarisation in PSN1 and BxPC3 cells. The extent to which Se compounds induced ROS production was substantially higher in the K-Ras mutated PSN1 cells than in the K-Ras wild-type BxPC3 cells. In particular, MSA treatment induced the highest level of ROS in PSN1 cells, approximately 6 times higher than the basal level after 90 minutes of incubation. In BxPC3 cells, however, MSA treatment only resulted in a slight increase in ROS production after 90 minutes of incubation (less than 2 times the basal level). Moreover, substantial ROS generation was detectable after 15-30 minutes of MSA treatment in PSN1 cells, while it was only detectable after 60 minutes in BxPC3 cells. Similarly, after 90 minutes of incubation with Sec, the level of ROS was approximately 4 times higher than the basal level in PSN1 cells, which was comparable to the antimycin treatment. In BxPC3 cells, however, the ROS level was only slightly elevated after 90 minutes of Sec treatment (less than 2 times the basal level). After 90 minutes of incubation with MSC, the level of ROS production was slightly elevated in PSN1 cells, approximately double that of the basal level. In BxPC3 cells, however, there was no detectable increase in ROS production after 90 minutes of incubation with MSC. After 90 minutes of incubation with selenite, the levels of ROS production were approximately 4 times and 2 times higher than the basal levels in PSN1 and BxPC3 cells, respectively. Interestingly, selenite was the most potent ROS inducer in BxPC3 cells.

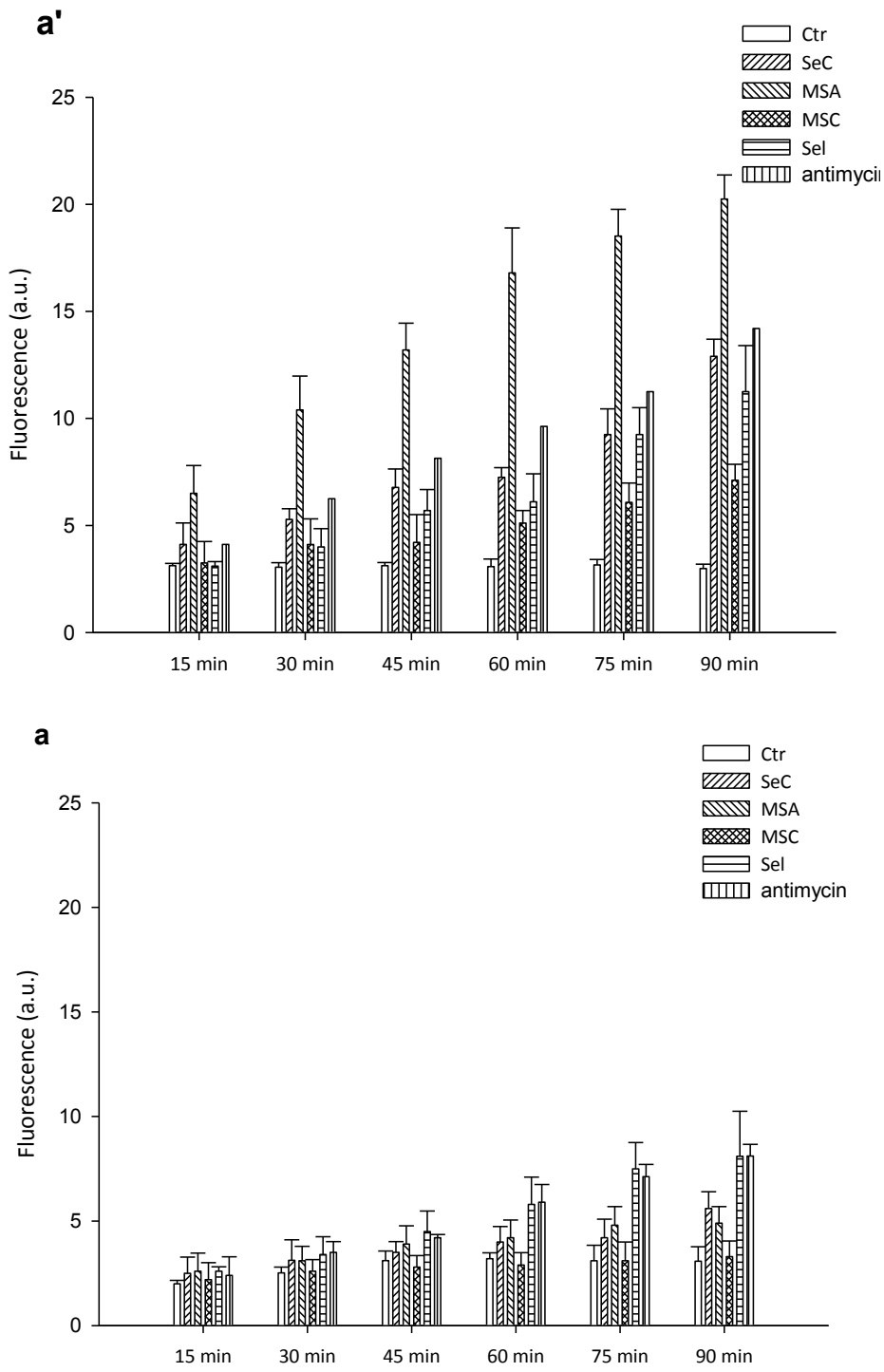

ROS production in PSN1 (a') and BxPC3 (a) cells. Cells were pre-incubated in 10 mM CM-H2DCFDA in PBS/10 mM glucose solution for 20 min at 37 °C . Cells were then treated with equimolar (50 µM) concentrations of Se compounds or Antimycin (3 µM). The fluorescent DCF signal was measured using 485 nm (excitation) and 527 nm (emission). Data represents mean fluorescence ± S.D.

Treatment with MSA resulted in a higher percentage of PSN1 cells (22%) than BxPC3 cells (13%) that displayed mitochondrial membrane depolarisation. A similar trend was observed for treatment with Sec, albeit to a lesser extent, with a higher percentage of mitochondrial depolarisation in PSN1 cells (18%) than in BxPC3 cells (7%). Treatment with MSC resulted in only a small percentage of both PSN1 (4%) and BxPC3 (3%) cells that displayed mitochondrial depolarisation. Conversely, treatment with selenite resulted in a significantly higher number BxPC3 cells (11%) than PSN1 cells (6%) that displayed mitochondrial depolarisation.

It is well established that Se compounds, by means of their redox active metabolites, have the potential to generate ROS through redox cycling of selenolates with GSH, the thioredoxin and glutaredoxin systems, as well as oxygen, which results in the production of superoxide and hydrogen peroxide. This ultimately generates oxidative stress and induces a cellular stress response. On this basis, we evaluated and compared the ability of Se compounds to induce oxidative stress in PSN1 and BxPC3 cells. MSA was not only the most cytotoxic compound in K-Ras mutated PSN1 cells, it was also the most potent inducer of oxidative stress and mitochondrial membrane depolarisation, followed by SeC, and then MSC. Conversely, in BxPC3 cells, ROS levels were not significantly elevated following treatment with organic Se compounds and their effects on mitochondrial membrane depolarisation were notably lower than those observed in PSN1 cells. Moreover, selenite was the most potent ROS inducer in BxPC3 cells and was equally as effective as MSA at disrupting the mitochondrial membrane potential. Additionally, histological analysis of PSN1 cells treated with organic Se compounds revealed clear signs of mitochondrial swelling and disruption to the ultrastructure of mitochondrial cristae. Ultimately, Se-treated PSN1 cells exhibit clear signs of oxidative stress in the mitochondria, which is typically associated with mitochondrial-mediated apoptosis. Importantly, this finding is in line with previous work demonstrating an increased susceptibility to oxidative stress in cells with K-Ras mutations.

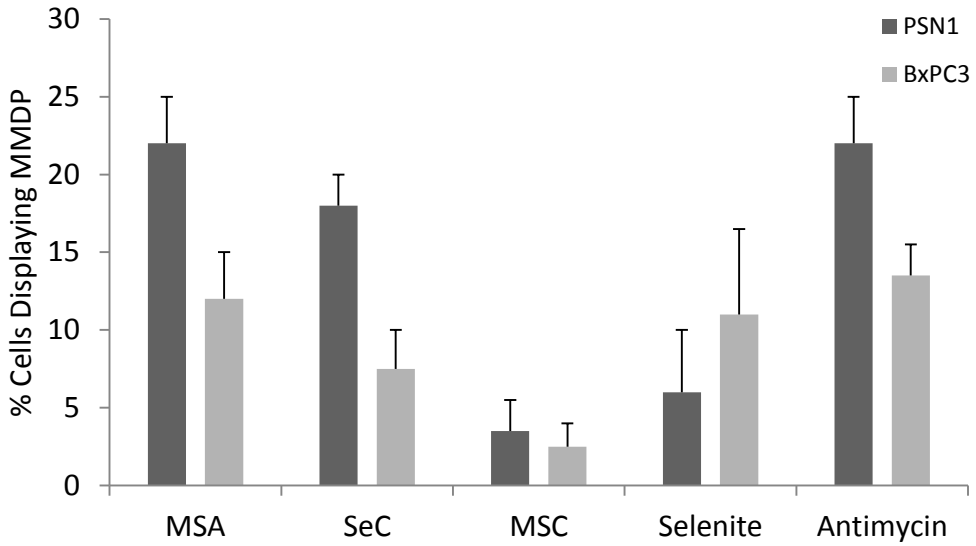

Mitochondrial membrane depolarisation (MMDP) in PSN1 and BxPC3 cells. Cells were treated with equimolar (50 µM) concentrations of Se compounds or Antimycin (3 µM) and then stained with JC-1 dye. The red-to-green (590nm/529nm) fluorescence intensity ratio was used to determine the percentage of cells displaying mitochondrial membrane depolarisation. Data represents the means ± S.D.

3.4 Antioxidant Enzyme Activity

Since Se compounds are redox active at high concentrations and drive the generation of oxidative stress, we assessed the capacity of both K-Ras mutated PSN1 cells and K-Ras wild-type BxPC3 cells to up-regulate their antioxidant defences by measuring the activity of three critical antioxidant enzymes, TrxR, GR and GPx.

Initially, the basal levels of enzyme activity were determined in untreated PSN1 and BxPC3 cells. PSN1 cells displayed higher levels of basal enzyme activity than BxPC3 cells. Specifically, the activity of TrxR, GR and GPx were approximately 2, 3 and 4 times higher in PSN1 than BxPC3 cells, respectively.

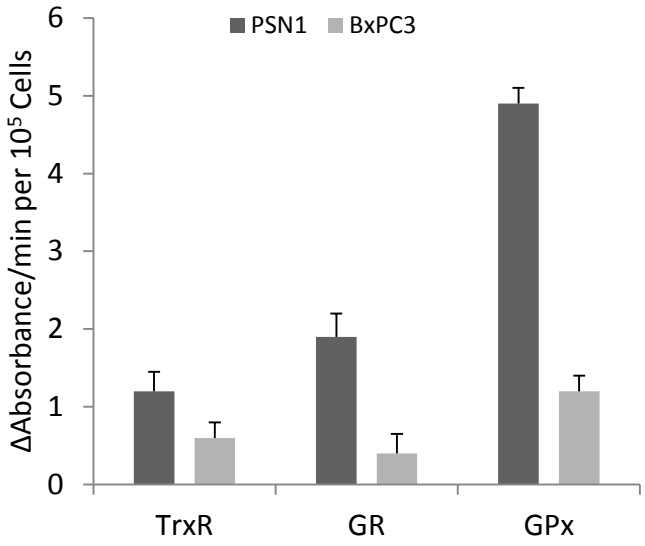

Basal levels of antioxidant enzyme activity in cell lysates extracted from PSN1 and BxPC3 cells. Data represents the mean change in absorbance per minute for 10^5 cells in enzyme activity assays for TrxR (412nm, DTNB reduction), GR (412nm, DTNB reduction) and GPx (340nm, NADPH consumption) ± S.D.

Given the differences in basal cellular antioxidant enzyme activity, it was of interest to determine whether the varying cytotoxicity of Se compounds across cell lines was associated with the capacity of cells to up-regulate their antioxidant defence. Although to varying extents for TrxR, GR and GPx, treatment with all Se compounds (2.5µM, 24 hours) resulted in a substantial increase in enzyme activity in BxPC3 cells compared to untreated controls. In particular, MSA-treated BxPC3 cells, displayed a 2.50-, 2.34- and 2.37-fold increase in TrxR, GR and GPx activity, respectively. Similarly, Sec-treated BxPC3 cells displayed a 1.78-, 1.67- and 2.97-fold increase, and MSC-treated BxPC3 cells displayed a 1.76-, 1.20- and 1.69-fold increase in TrxR, GR and GPx activity, respectively. These effects were comparable to those elicited by selenite treatment, which induced a 1.62-, 1.52- and 2.83-fold increase in TrxR, GR and GPx activity, respectively, in BxPC3 cells. Conversely, the effect of Se compound treatment (2.5 µM, 24 hours) on antioxidant enzyme activity levels in PSN1 cells was not as pronounced as that observed in BxPC3 cells. In general, for all Se compounds and for all antioxidant enzymes, there was only a minor increase (1.1-1.3-fold) in enzyme activity compared to untreated controls.

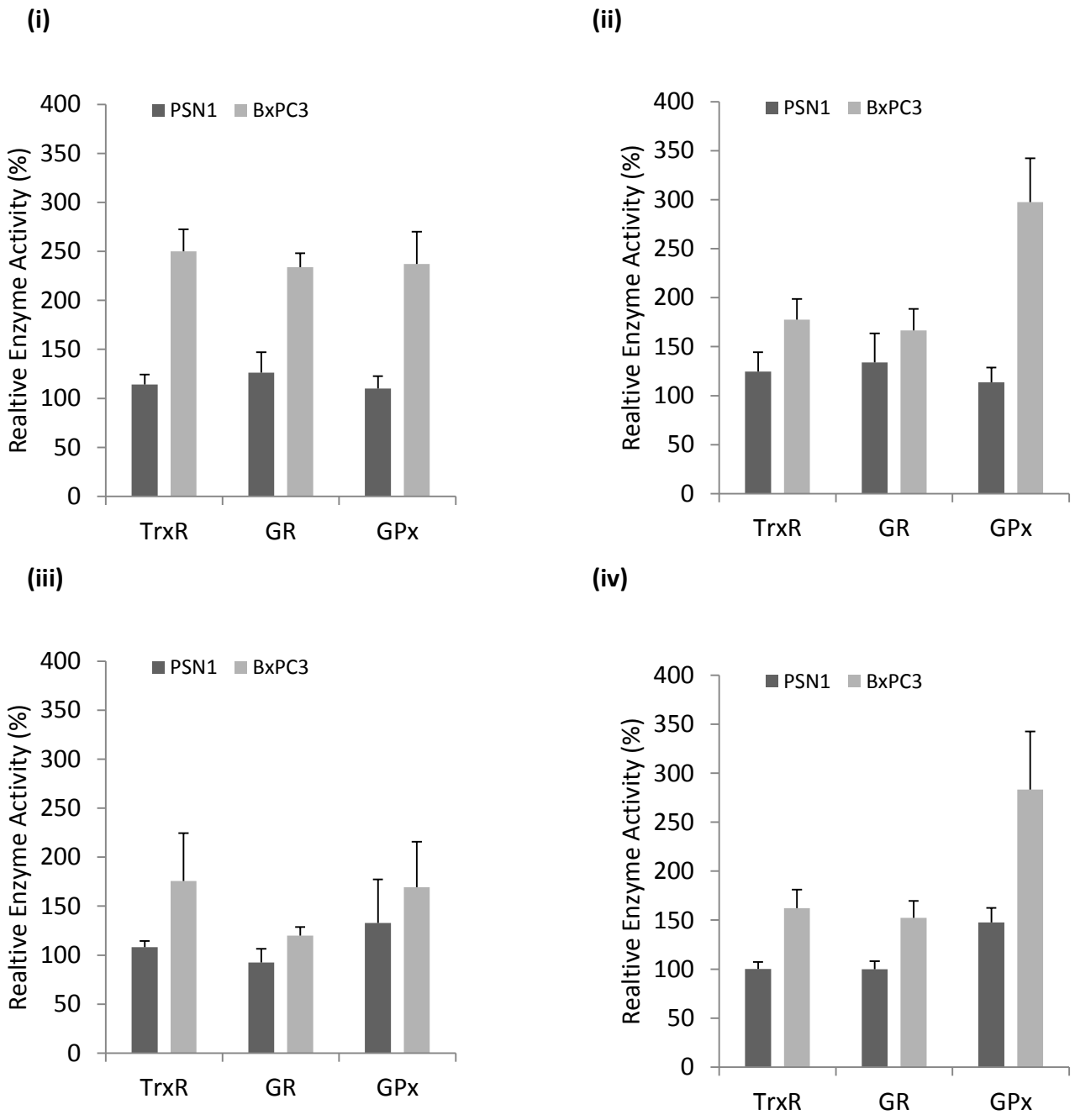

Antioxidant enzyme activity in cell lysates extracted after 24 hours of Se compound treatment. Data represents the mean relative activity (compared to untreated controls) of TrxR, GR and GPx in PSN1 and BxPC3 cells treated with (i) MSA, (ii) SeC (iii) MSC and (iv) Selenite ± S.D.

In order to examine the immediate antioxidant response to Se compound treatment, the activity of TrxR was also performed after 5 hours. For both BxPC3 (1.06 – 1.51) and PSN1 cells (1.07 – 1.34), the level of antioxidant enzyme activity was either modestly higher than or similar to that of untreated control cells. Considering the cellular responses after both 24 hours and 5 hours of treatment, it is clear that in BxPC3 cells Se compounds induced a time-dependent increase in antioxidant enzyme activity levels, whereas, in PSN1 cells the induced enzyme activity was comparably low at both time points.

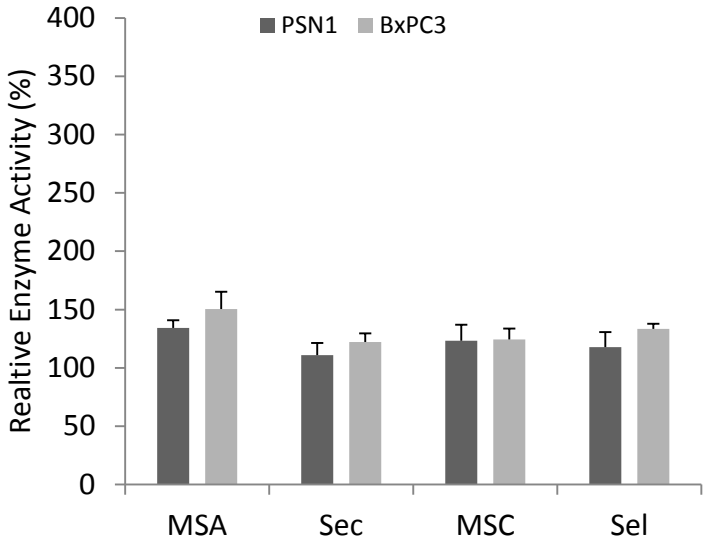

Antioxidant enzyme activity in cell lysates extracted after 5 hours of Se compound treatment. Data represents the mean relative activity (compared to untreated controls) of TrxR in PSN1 and BxPC3 cells treated with (i) MSA, (ii) SeC (iii) MSC and (iv) Selenite ± S.D.

In addition to the differences observed across cell lines in ROS generation and ROS-mediated cellular damage, the antioxidant stress response of PSN1 and BxPC3 cells was markedly different. Importantly, PSN1 cells displayed substantially higher basal activity levels than BxPC3 cells for the critical antioxidant enzymes, TrxR, GR and GPx. However, after treatment with Se compounds, BxPC3 were able to upregulate the activity of these enzymes, while PSN1 cells were not. Most likely, the high basal levels of antioxidant enzyme activity in PSN1 cells allowed very little room for the induction of an antioxidant response. On the other hand, BxPC3 cells, which have lower basal levels of antioxidant enzyme activity, were able to adapt to oxidative stress by up-regulating their antioxidant defence,

making them more resistant to oxidant treatment. This finding supports the theory that protection against oxidative stress is determined by the ability to induce an antioxidant response as opposed to the basal level of antioxidant activity. In this sense, PSN1 cells can be considered “maximised” in regard to their antioxidant defence, while BxPC3 cells have a greater capacity to adapt to oxidative stress.

It is interesting to point out that if tolerating high basal levels of ROS production through the up-regulation of antioxidant defences is a central facet of tumour cell survival, it follows that treatment with antioxidants would aid tumour cell proliferation. Indeed, in an inducible oncogenic K-Ras mouse model of lung cancer, treatment with antioxidants has been shown to disrupt the ROS-p53 pathway and accelerate tumour growth[104]. Likewise, in an inducible oncogenic BRAF mouse model of melanoma, treatment with antioxidants has been shown to increase tumour metastases through enhanced migration signalling[105]. It has further been shown that successful metastasis of patient-derived melanoma cells in NSG mice is dependent upon an increased capacity of tumour cells to tolerate oxidative stress through an increased dependence on NADPH-generating enzymes[106]. Hence, while tolerating higher basal levels of ROS is an adaptation of cancer cells that is essential to their survival and proliferation, it leaves them vulnerable to additional oxidative stress. Therefore, Se compound derived oxidants provides a potential means to specifically target cells, such as K-Ras mutated pancreatic cancer cells, that have elevated basal levels of ROS production.

3.5 Antioxidant Enzyme mRNA Expression

Given the notable differences observed between PSN1 and BxPC3 cells in their antioxidant enzyme activity after 24 hours of treatment with Se compounds, we investigated the cellular antioxidant response at the level of mRNA expression both immediately, after 6 hours, and after the induced change in enzyme activity levels, after 24 hours. In this manner, we were able to decipher whether the differences observed between PSN1 and BxPC3 cells in their ability to induce an antioxidant response were due to their relative capacity to alter gene expression.

The increased expression of TXNRD1 after 6 hours of treatment with MSA is a strong indicator that both PSN1 and BxPC3 cells are undergoing an oxidative stress response. In agreement with our previous findings, MSA appears to be a more potent pro-oxidant than selenite and thus induced a stronger response at the level of mRNA expression. It is interesting to note that there was little change in TXNRD1 expression levels after treatment with selenite in either cell line. This is surprising, as selenite is a well-established redox active Se compound. After 24 hours of treatment, there were no substantial (greater than 2-fold) increases in the expression of downstream NRF-2 targets. Expression of TXNRD1 was slightly elevated (albeit less than 2-fold) in PSN1 cells, but not in BxPC3 cells, treated with MSA.

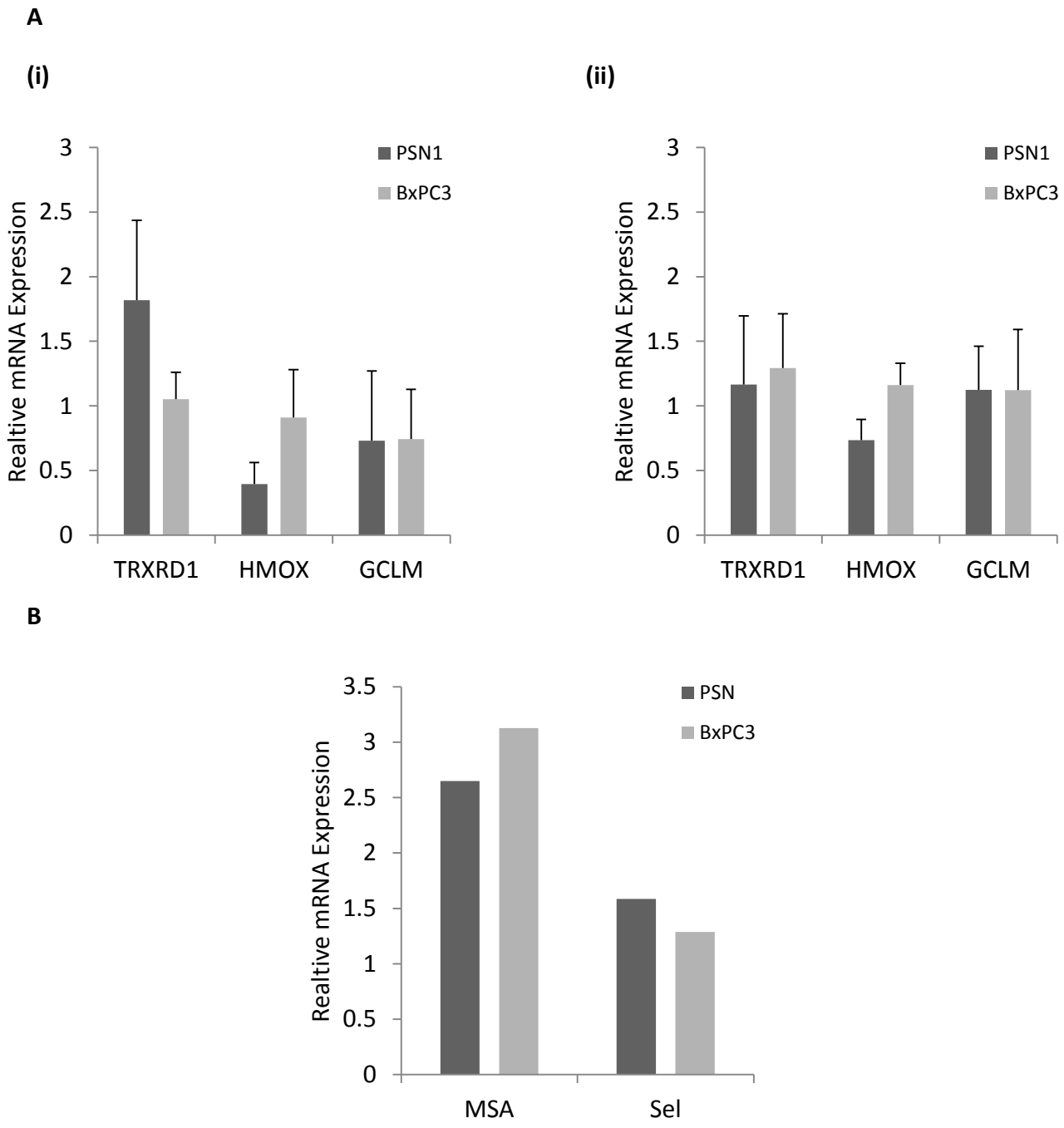

mRNA expression of NRF-2 downstream targets in PSN1 and BxPC3 cells treated with MSA and selenite. (A) The relative expression (compared to untreated cells) of TXNRD1, HMOX and GCLM after 24 hours of treatment (2.5µM) with (i) MSA and (ii) Selenite. (B) The relative expression of TXNRD1 after 6 hours of treatment (5µM) with MSA and selenite. Data represents the mean relative expression.

In order to examine the cellular antioxidant response at the gene transcription level, we performed RT-qPCR on MSA-treated and selenite-treated PSN1 and BxPC3 cells. Specifically, we investigated several downstream targets of the transcription factor NRF-2 [Nuclear

factor (erythroid-derived 2)-like 2], which is considered the master regulator of the cellular antioxidant response. The target genes included (1) the antioxidant enzyme, TrxR (TXNRD1); (2) the glutamate–cysteine ligase complex modifier subunit (GCLM), which is involved in the glutathione production/regeneration pathway; and (3) haem oxygenase (HMOX), a reductive enzyme involved in iron sequestration. After 6 hours of treatment with MSA, both PSN1 and BxPC3 cells displayed a similar increase (2.5-3 times) in the level of TXNRD1 mRNA, which suggests that both cell lines initiated an antioxidant stress response. However, this response was not observed following selenite treatment, which was surprising. After 24 hours of MSA treatment, there was a minor increase in TXNRD1 expression in PSN1 cells, but not in BxPC3 cells. Taken together with the enzyme activity after 24 hours, it is plausible that antioxidant gene expression is an immediate response, while antioxidant enzyme activity persists over time, following protein assembly. Hence, while both cell lines displayed a transient increase in TXNRD1 expression after 6 hours, it appeared that only BxPC3 cells were capable of translating this into a functional antioxidant response, while PSN1 cells were not. This may also explain why PSN1 cells continued to express elevated levels of TXNRD1 after 24 hours, while BxPC3 cells did not.

Our findings in pancreatic cancer cells are in agreement with previous studies that support the hypothesis that Se-derived pro-oxidant therapy targets the capacity, or lack thereof, of cells to up-regulate their antioxidant defences. Several drug-resistant lung cancer cells were shown to display higher basal TrxR activity levels and lower up-regulation of their TrxR activity following selenite treatment than their drug-sensitive variants[47,61]. Similarly, lung cancer cells treated with increasing doses of selenite displayed a dose-dependent increase in TrxR mRNA expression despite their being no increase in TrxR protein or activity levels at the highest treatment concentrations, suggesting an inhibition or “maximisation” of protein synthesis[48]. Similarly, in multi-drug resistant primary acute myeloid leukemia cells, selenite treatment was shown to increase TrxR and Grx mRNA expression, but this was not reflected by any increase in TrxR protein levels[54]. In addition, the toxicity of auranofin, an established TrxR inhibitor, was shown to be potentiated by pre-incubation with selenite[51]. Since it appears that the reduced capacity to up-regulate antioxidant defence is associated with higher susceptibility to selenite, it follows that the contrary is also true. Indeed, the virally transduced overexpression of mitochondrial superoxide dismutase has been shown to

inhibit superoxide production and apoptotic cell death in prostate cancer cells treated with selenite[49].

3.6 Transmission Electron Microscopy

In order to visually examine the effects of Se compounds on cellular ultrastructure, we performed TEM on PSN1 cells. MSA treatment induced dramatic swelling of the mitochondria (increased volume), which is associated with decreased electron density of the inner mitochondrial membrane and mitochondrial matrix. Similarly, Sec and MSC treated cells displayed mitochondrial swelling and disrupted mitochondrial cristae. Control cells, on the other hand, displayed intact, electron-dense mitochondria.

(a)

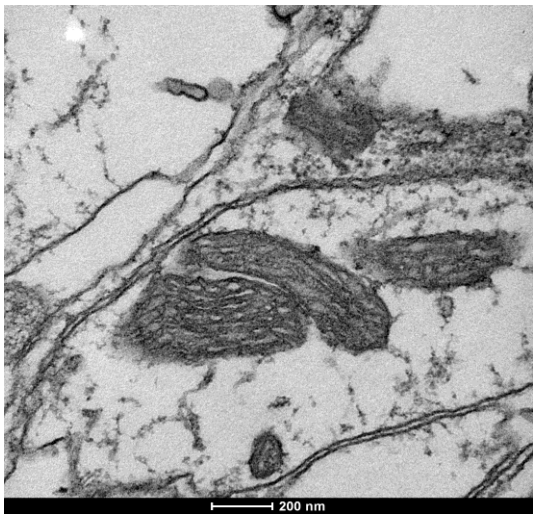

(b)

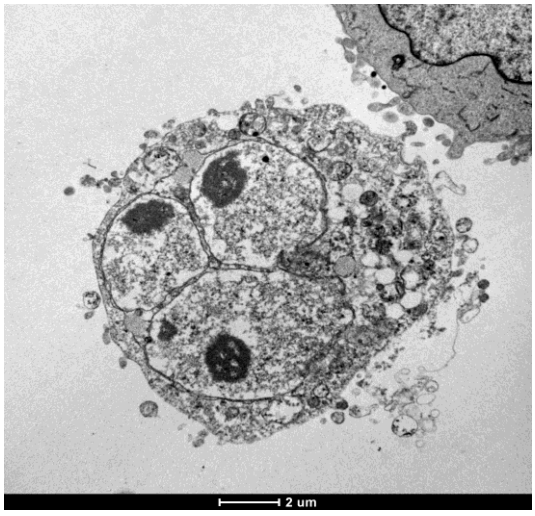

(c)

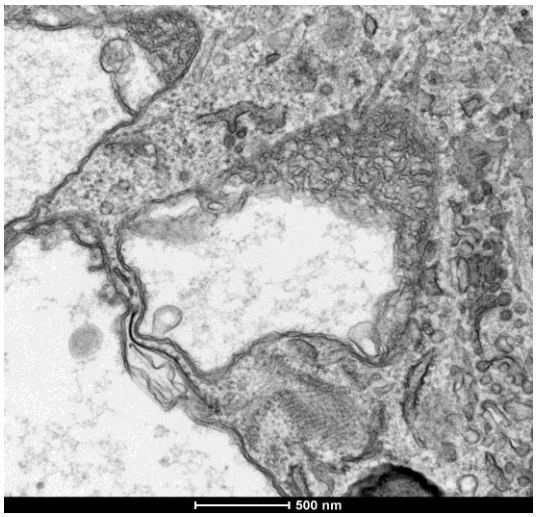

(d)

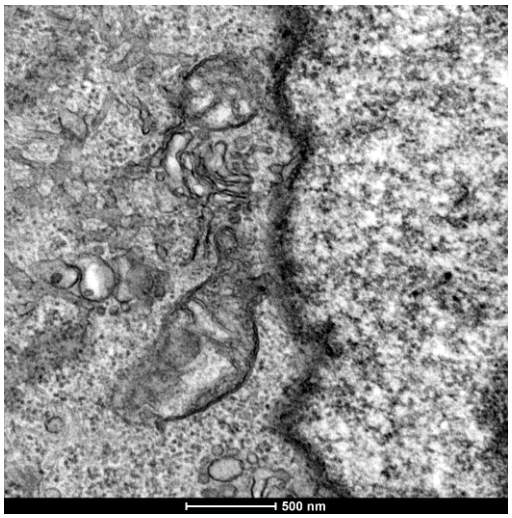

(e)

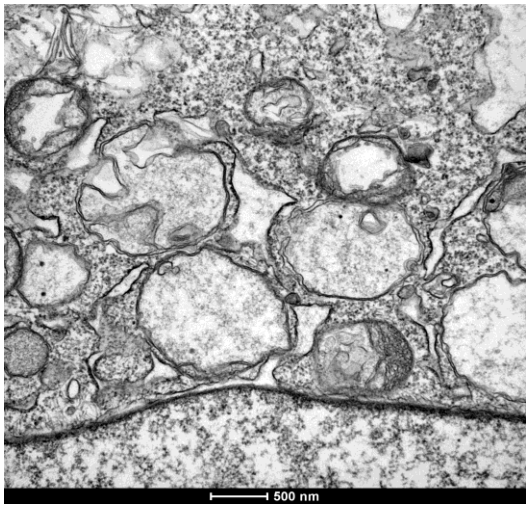

(f)

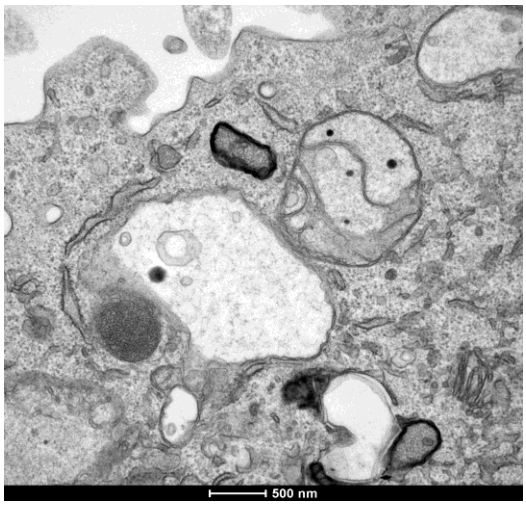

TEM images of PSN1 cells treated for 24 hours with their respective IC_{50} concentrations (as determined by MTT) of Se compounds. Control cells (a); MSA treated cells (b) and (c); SeC treated cells (d); MSC treated cells (e); and selenite treated cells (f).

3.7 *In Vitro* DNA Interactions

In order to investigate the potential genotoxic effects of Se compounds, we performed two DNA interaction assays: (1) the CT-DNA interaction assay to test for direct interaction with linear DNA, which would be detectable by a spectral absorbance shift, and (2) the pUC19 plasmid cleavage assay to test for direct changes to the structure of supercoiled plasma DNA, which would be detectable through gel electrophoresis.

3.7.1 CT-DNA Interaction Assay

As it has been previously observed, no differences were observed between the UV spectra of CT-DNA incubated with organic Se compounds and untreated DNA. This suggests that none of the compounds were able to interact with DNA *in vitro*.

3.7.2 pUC19 Cleavage Assay

After treatment with all organic Se compounds, pUC19 remained primarily in its supercoiled form. This suggests that none of the compounds were able to directly alter the structure of DNA *in vitro*.

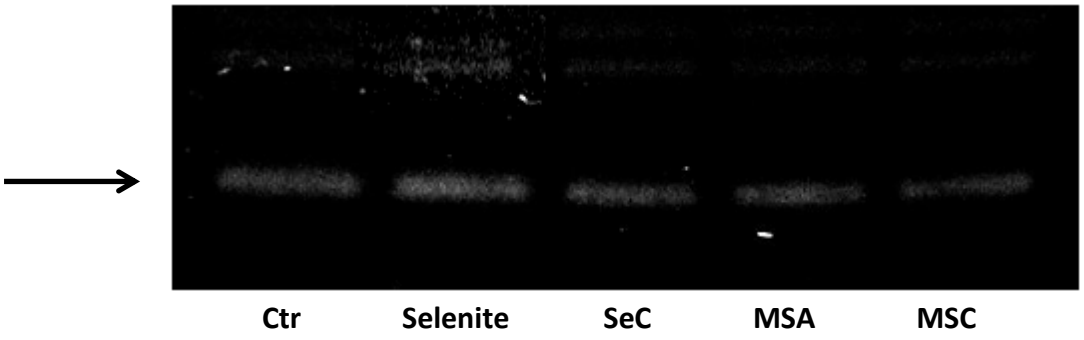

Gel electrophoresis of pUC19 plasmids incubated for 3 hours with organic Se compounds (50µM) and selenite (50µM). The arrow indicates the band representing the supercoiled form (form 1) of the plasmid.

3.8 In Vivo Effects of MSA

Given both the higher potency of MSA than selenite in vitro and the potentially lower systemic toxicity of organic Se compounds than selenite, it was important to investigate whether these same effects could be observed in vivo. Using a LLC model, MSA treatment resulted in both a greater reduction of tumour mass (90% vs. 85%) and a lower reduction in body weight (12% vs 18%) compared to selenite treatment. This ultimately confirmed the above-mentioned findings in cell-based and in vitro experiments that MSA has a higher potency and lower systemic toxicity than selenite. Importantly, the reduction of tumour mass associated with MSA treatment was comparable to that of Cisplatin and also resulted in a lower change in body mass after 7 days of treatment.

	Daily dose *i.p.* (mg/kg)	Tumour weight (g) (mean ± S.D.)	Inhibition of tumour growth (%)
Control		0.598±0.11	
Selenite	3	0.089±0.02	84.8
MSA	3	0.058±0.02	89.7
CDDP	3	0.063±0.01	89.5

[a] vehicle only (saline)

LLC tumour weight in the hind legs of C57BL mice following treatment with MSA, selenite or vehicle (alone). Treatment began on day 7 post tumour injection, when visible tumours had formed. IP chemotherapy treatment was given daily from day 7 to day 14.

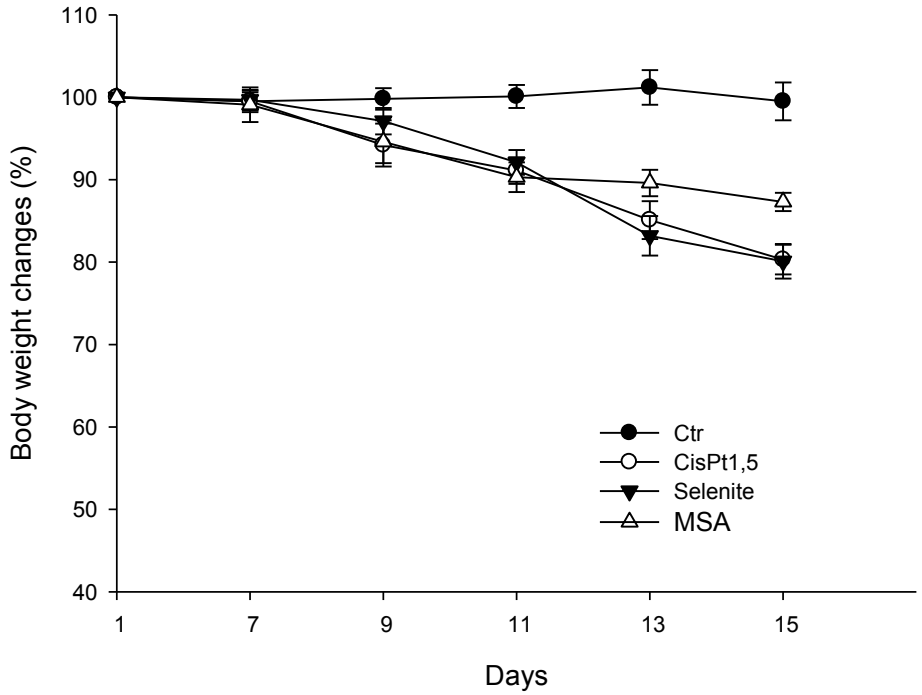

The body weight changes of LLC-bearing C57BL mice treated with MSA, selenite, CDDP or vehicle alone. Data represents the mean body weight ± S.D. relative to the mean weight on day after tumour injection.

Despite the ability of selenite to effectively kill cancer cells through the induction of redox stress, it is known to cause ROS-mediated DNA strand breaks that can lead to chromosomal damage in both cancer cells and non-transformed cells. This potential for genotoxicity increases the systemic toxicity of selenite and thus limits its therapeutic potential. It is also an important consideration with regards to the risk of developing secondary malignancies in patients. Hence, it is of great therapeutic relevance to investigate other Se compounds that possess lower systemic toxicity. The higher potency, as measured by a reduced tumour mass, and the lower systemic toxicity, as determined by a smaller change in body weight, of MSA than selenite in the LLC mouse model are strong indicators that MSA has a greater therapeutic potential than selenite.

4 Results (Part 2): Tyrosine Kinase Inhibitor Se Derivatives

As stated previously, there is a requirement for more effect treatments for PC. The second part of this thesis focuses on assessing the therapeutic potential of three novel Se derivatives, GY811, GY812 and GY813, of the tyrosine kinase inhibitors (TKIs) Imatinib, Dasatinib and Sorafenib, respectively. Since TK dysregulation is a common feature among different types of cancers, the synthesis of dual-action, multi-targeted Se derivatives of TKIs offers the potential to treat additional types of cancer than those already clinically approved for the parental compounds. The incorporation of a Se moiety into the structure of TKIs potentially renders the Se derivatives redox active, on top of their inhibitory activity toward TKs. While the effects of TKIs have not been extensively studied in PC, their TKI Se derivatives may be even more potent in cells that are susceptible to oxidative stress, such as K-Ras mutated PC cells. The findings of this study will shed light on the potential use of Se derivatives of existing chemotherapy drugs for use in the treatment of PC.

4.1 Cell Viability Assays

In order to examine and compare the potency of TKI Se derivatives with their reference compounds, cytotoxicity was measured in a panel of pancreatic cancer cell lines by means of the MTT cell viability assay. All Se derivatives, GY811, GY812 and GY813, were more potent than their respective reference compounds, Imatinib, Dasatinib and Sorafenib across pancreatic cancer cell lines. Specifically, in K-Ras mutated PSN1 cells, the IC50 values for GY811 (3-fold), GY812 (>50-fold) and GY813 (3-fold) were substantially lower than those of their reference compounds. Similarly, in K-Ras mutated PANC1 cells, the IC50 values for GY811 (1.8-fold), GY812 (5-fold) and GY813 (1.86-fold) were lower than those of their reference compounds. In K-Ras wild-type BxPC3 cells, however, the IC50 values for GY811 (1.8-fold), GY812 (2.6-fold) and GY813 (1.8-fold) were generally only slightly lower than those of their reference compounds. It is interesting to note that in non-transformed HEK293 cells, the IC50 values for GY811 (1.17-fold lower), GY812 (1.76-fold lower) and GY813 (1.08-fold) were comparable to those of their reference compounds.

	MTT IC_{50} (µM ± S.E.)					
	Imatinib	GY811	Dasatinib	GY812	Sorafenib	GY813
PSN1	5.21 ± 1.13	1.74 ± 0.59	11.76 ± 1.53	0.22 ± 0.04	6.28 ±2.96	1.99 ± 0.58
BxPC3	3.73 ± 0.64	2.06 ± 1.43	6.54 ± 3.93	2.47 ± 0.84	4.56 ± 1.11	2.50 ± 1.02
PANC1	2.47 ± 0.70	1.35 ± 0.54	5.39 ± 1.35	1.02 ± 0.40	2.06 ± 0.42	1.11 ± 0.48
HEK293	5.00 ± 0.53	4.25 ± 0.17	2.41 ± 0.49	1.95 ± 0.83	4.87 ± 0.31	4.49 ± 0.70

Cytotoxicity of tyrosine kinase inhibitor Se derivatives in PSN1, PANC1, BxPC3 and HEK293 cells. Cells were treated for 72 hours with increasing concentrations of Se derivatives in parallel with their reference compounds. Cytotoxicity was assessed by the MTT and IC_{50} values were calculated by a four parameter logistic model. Data represents the means ± S.D.

All TKI Se derivatives displayed lower IC_{50} values than their reference compounds in PSN1, PANC1 and BxPC3 cells. Interestingly, the relative cytotoxicity of Se derivatives compared to their reference compounds was greater in the K-Ras mutated PSN1 and PANC1 cells than in the K-Ras wild-type BxPC3 cells. Moreover, in non-transformed HEK293 cells, Se derivatives were only slightly more potent than their reference compounds. Hence, the introduction of a selenium moiety to TKIs increased their cytotoxic potential as well as their selectivity for both K-Ras mutated pancreatic cancer cells over K-Ras wild-type pancreatic cancer cells and for transformed cells over non-transformed cells. This is a significant finding as it highlights the potential of dual-action Se derivatives to more specifically target tumour cells than their reference compounds. Ultimately, this may have clinical implications such as a lower risk or severity of side-effects.

4.2 Cellular Uptake

With the aim of determining the correlation between cytotoxicity and intracellular accumulation of Se derivatives, GF-AAS was performed on the cellular contents of BxPC3 and HEK293 cells treated with GY811, GY812 and GY813. Cellular uptake was higher in BxPC3 than in HEK293 for all Se derivatives. In particular, GY812 accumulation was about 6 times higher in BxPC3 than in HEK293, while GY811 and GY813 accumulation was about 1.5 times higher in BxPC3 cells.

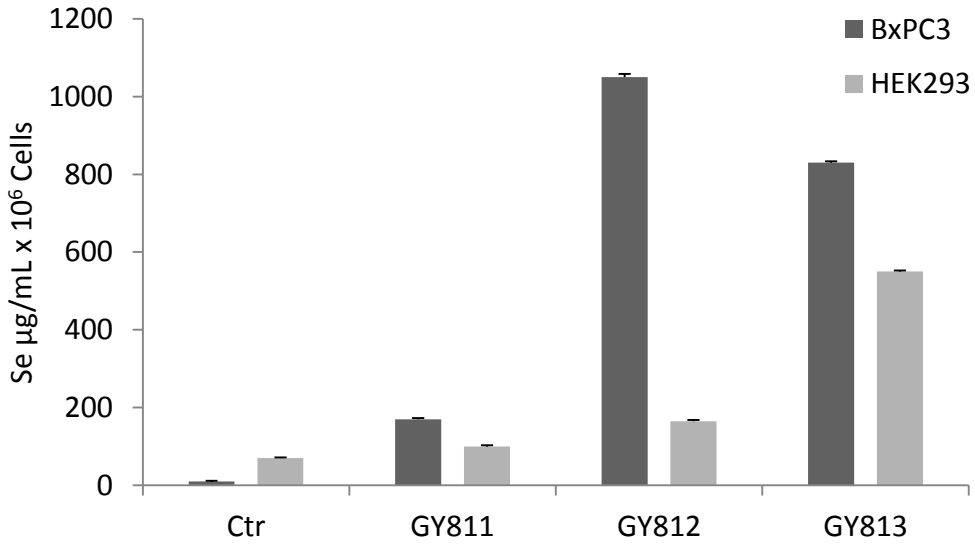

Cellular uptake of TKI Se derivatives in BxPC3 and HEK293 cells. Cells were incubated with Se derivatives (10 µM) for 24 hours. The cellular Se content was determined by means of GF-AAS analysis. Data represents the means ± S.D.

The cellular Se accumulation was notably higher in BxPC3 cells than in HEK293 cells for all TKI Se derivatives, which correlates with the relative cytotoxicity of the compounds across cell lines. Hence, the cellular uptake of Se derivatives may partly account for their increased selectivity toward pancreatic cancer cells over non-transformed cells. In future studies, it will be interesting to see if Se derivatives show a higher selective uptake than their respective reference compounds.

4.3 ROS Production

Since organic Se molecules are usually redox active, GY811, GY812 and GY813 were synthesized with the aim of incorporating a redox active Se moiety into their parental compounds, which function as tyrosine kinase inhibitors. To determine whether the metabolism of Se in these novel TKI derivatives has the potential drive the generation of ROS, ROS production was measured after treatment with Se derivatives and compared to that of their reference compounds. All Se derivatives induced higher levels of ROS production (approximately 25%, 50% and 30% for GY811, GY812 and GY813, respectively) compared to their respective reference compounds. Hence, for all three Se derivatives, the addition of a Se moiety renders the compound more redox active, which may also account for their enhanced cytotoxicity.

(a)

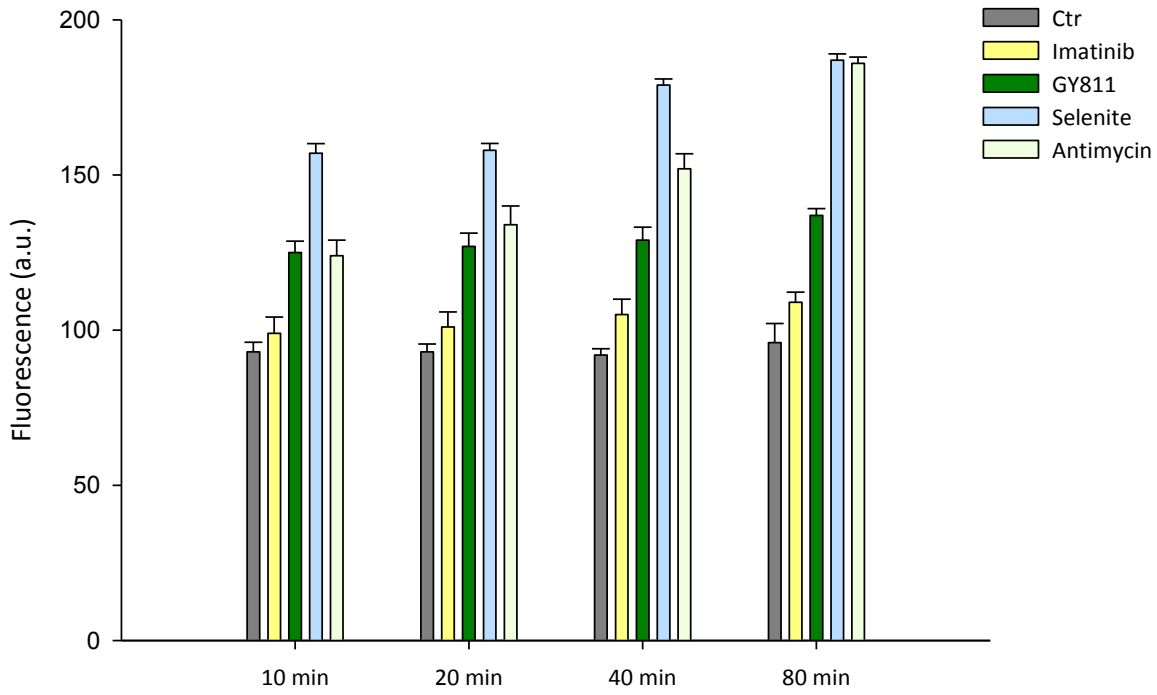
Fluorescence (a.u.)
200
150
100
50
0
10 min
20 min
40 min
80 min
Ctr
Imatinib
GY811
Selenite
Antimycin

(b)

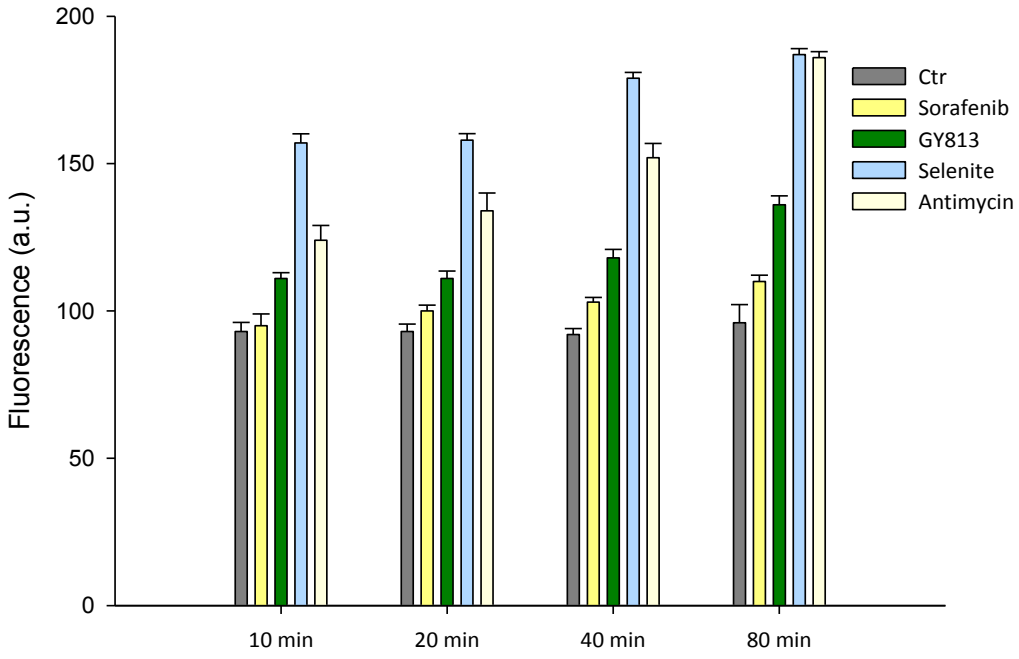
Fluorescence (a.u.)
200
150
100
50
0
10 min
20 min
40 min
80 min
Ctr
Sorafenib
GY813
Selenite
Antimycin

(c)

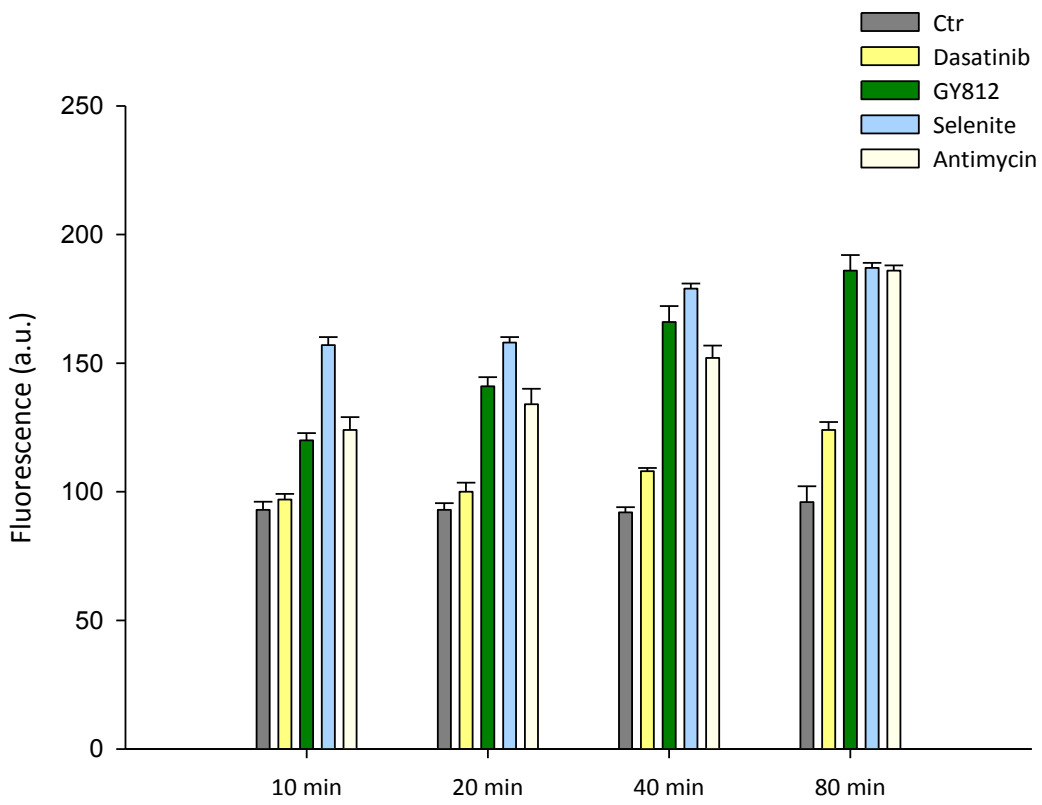

ROS production in BxPC3 cells following treatment (10µM) with (a) GY811 (b) GY812 and (c) GY813 and their respective reference compounds, Imatinib, Dasatinib and Sorafenib. Cells were pre-incubated in 10 mM CM-H2DCFDA in PBS/10 mM glucose solution for 20 min at 37 °C prior to treatment. The fluorescent DCF signal was measured using 485 nm (excitation) and 527 nm (emission). Data represents mean fluorescence ± S.D.

Treatment with the TKI Se derivatives GY811, GY812 and GY813, resulted in a higher level of ROS production in BxPC3 cells than treatment with their respective reference compounds. Although this increase in ROS production was minor (approximately 25-50%), it is still biologically relevant and, at least partly, contributes to the higher cytotoxicity of the Se derivatives than their reference compounds. Moreover, the induction of ROS may also account for the increased selectivity of the Se derivatives against K-Ras mutated cells, which are considered to be more susceptible to oxidative stress. In order to confirm this hypothesis, it will be necessary, in future studies, to compare the levels of ROS generation and markers of oxidative stress in PSN1, PANC1 and other K-Ras mutated cell lines after treatment with TKI Se derivatives.

In addition to the higher level of ROS generation that is linked to treatment with redox active Se molecules, the addition of a Se moiety to TKIs likely alters their affinity and/or specificity for the ATP binding site of kinases. While it is difficult to decipher these effects in cells, *In Vitro* analysis of kinase activity are currently being investigated. As dual-action Se derivatives, the combined effects of TK inhibition and acting as oxidants render these compounds more cytotoxic and selective than their reference compounds.

4.4 Cellular Free Thiols

Since Se compounds that are redox active are thought to result in the consumption of cellular thiols, we determined cellular thiol levels following treatment with TKI Se derivatives and their parental compounds. Treatment with all TKI Se derivatives and their reference compounds resulted in a significant decrease (25-60%) in the level of cellular free thiols. Interestingly, however, no substantial differences were seen between Se derivatives and their reference compounds.

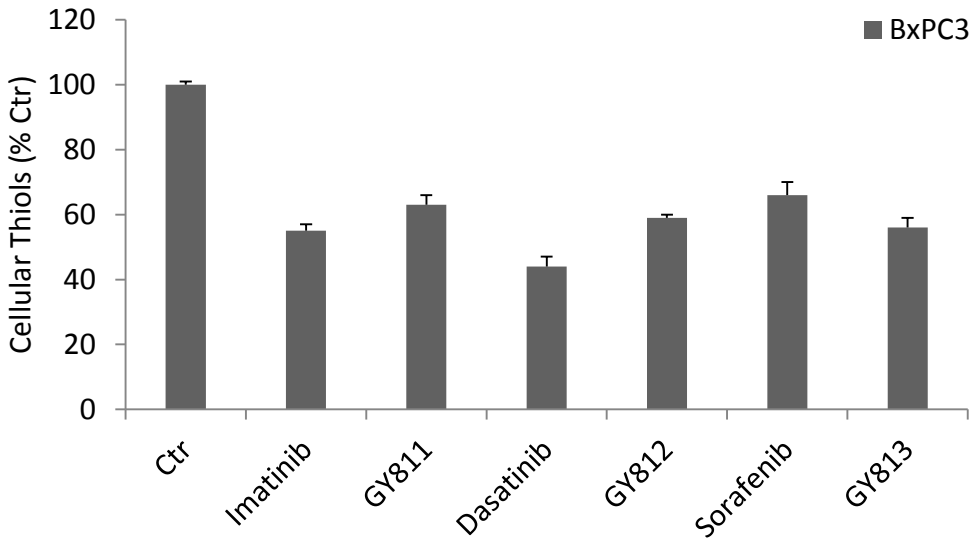

Relative availability of free thiols in BxPC3 cells treated with TKI Se derivatives and their reference compounds as determined by the DTNB assay. Data represents mean free thiol levels ± S.D relative to untreated controls.

Although TKI Se derivatives were more redox active than their reference compounds, this did not appear to affect the level of free thiols in BxPC3 cells. This suggests that the availability of free thiols is unlikely to be a major factor underlying the enhanced cytotoxicity of Se derivatives compared to their reference compounds. Nevertheless, this finding is surprising since oxidants typically act by consuming both protein bound and free thiols.

4.5 GY813 Activity in a 3D Spheroid Model of Resistant Glioma (#18) Cells

Of the three staining methods used, the combination of Hoechst 33258 and PI staining was the most successful. Representative images of a cross-section through the centre of spheroids are shown in part A of the figure below. Although the 3D spheroid staining analysis is yet to be performed, from the images it is apparent that treatment with GY813 results in stronger PI staining than with Sorafenib under both normoxic and hypoxic conditions, which indicates a higher level of cell death. This effect is most evident at the 15µM treatment, where spheroids treated with Sorafenib appear similar to untreated controls, while spheroids treated with GY813 show intense PI staining. Interestingly, the efficacy of either compound does not seem to be substantially altered under hypoxic conditions compared to normoxic conditions. Staining with lysotracker resulted in a high level of background, making it unclear whether it would be an accurate measure of cell viability (data not shown). Staining with the LOX-1 hypoxia marker failed to specifically stain cells. Hence it was unclear whether the staining had worked (data not shown).

The results of the CellTiter-Glo® assay are shown in figure 3B. The IC50 values determined for treatment with GY813 and Sorafenib were 49.1 and 34.4 µM respectively. These IC50 values are substantially higher than what we would expect to see by analyzing the spheroids stained with PI. While it is clear that PI penetrates the spheroid and stains cells in its core, it is not certain that the CellTiter-Glo® assay successfully measured the viability of all cells in the spheroid. Hence, the cell viability measured may only reflect that of cells on the outer regions of the spheroid, which were physically subjected to the CellTiter-Glo® reagent.

A (i)

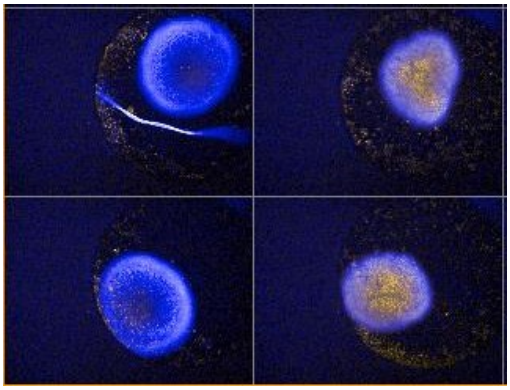

Ctr Selenite

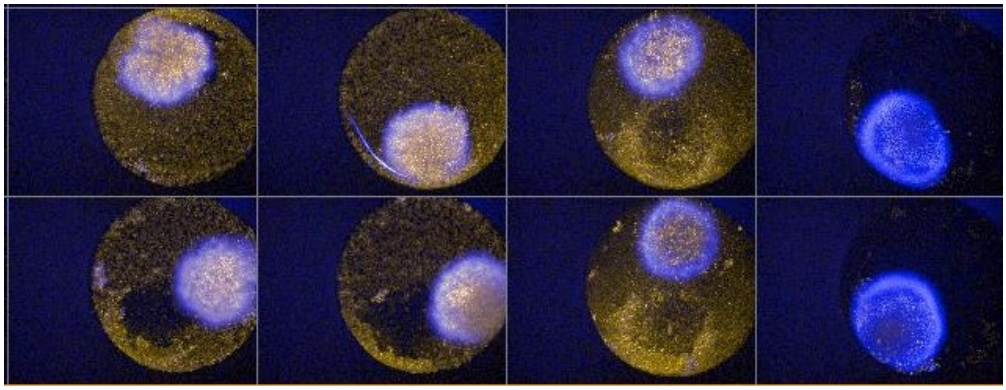

GY813 60μM GY813 45μM GY813 15μM GY813 7.5μM

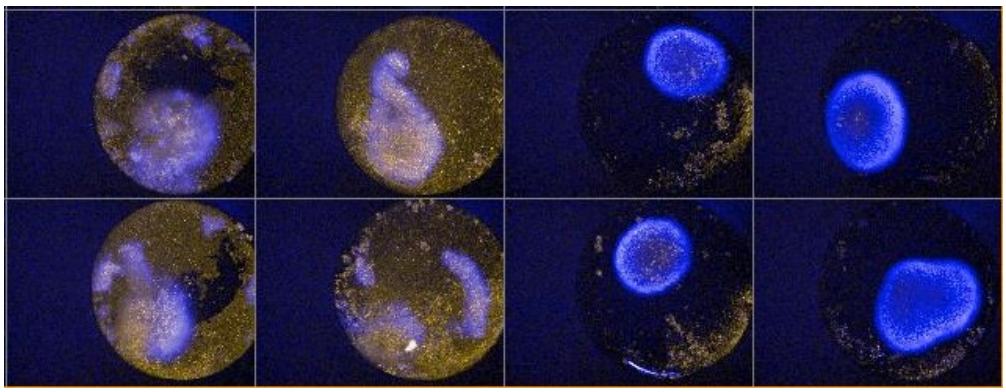

Sorafenib 60μM Sorafenib 45μM Sorafenib 15μM Sorafenib 7.5μM

(ii)

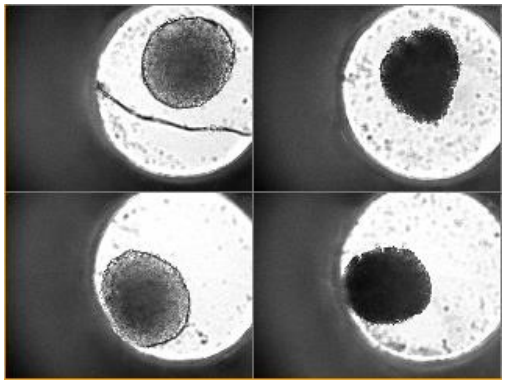

Ctr Selenite

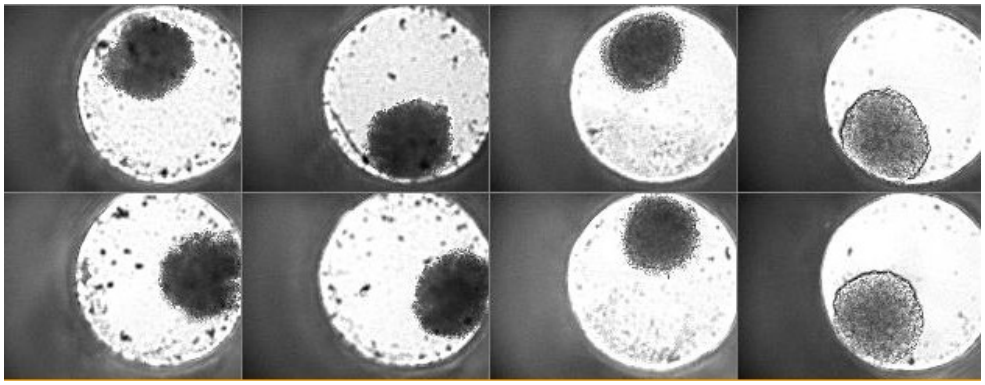

GY813 60μM GY813 45μM GY813 15μM GY813 7.5μM

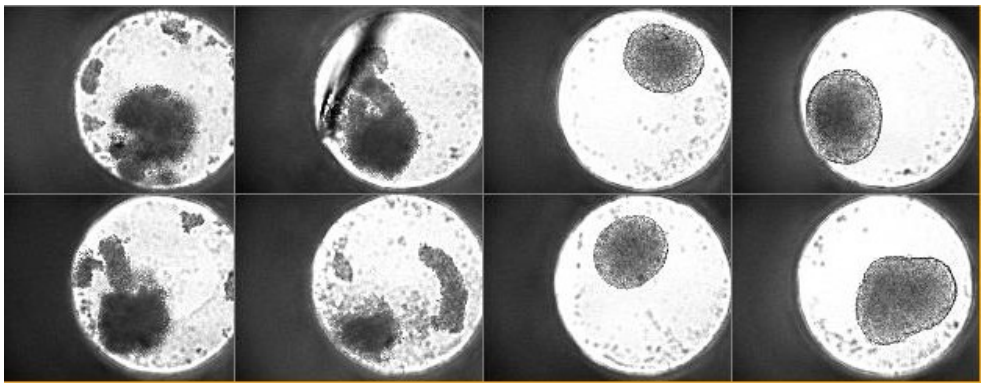

Sorafenib 60μM Sorafenib 45μM Sorafenib 15μM Sorafenib 7.5μM

B

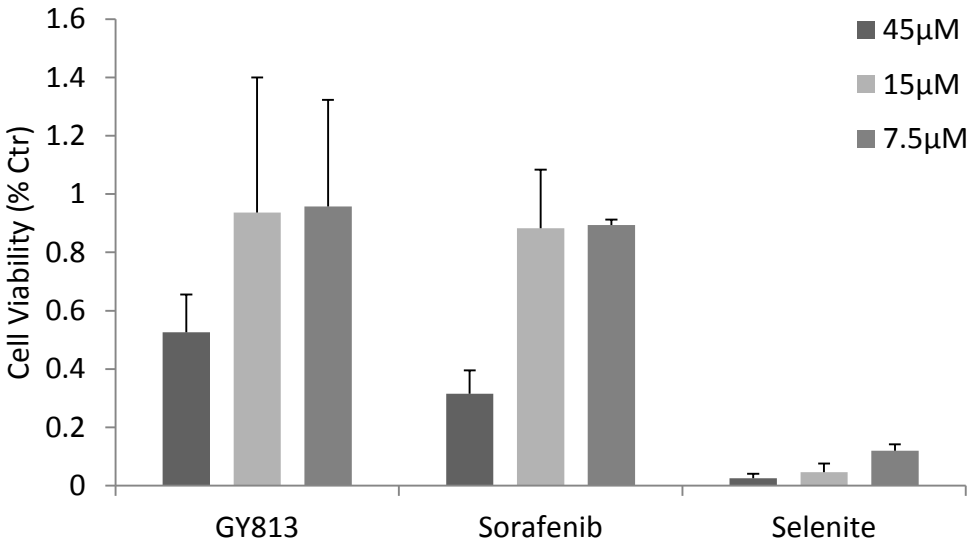

Cytotoxicity assays in Glioma #18 3D spheroids treated with increasing concentrations of GY813 and Sorafenib. (A) Representative cross-sections of spheroids stained with (i) Hoechst 33258 (blue) and propidium iodide (orange) and (ii) bright field images after treatment for 72 hours under normoxic conditions. (B) Relative cell viability as determined by the CellTiter-Glo® assay.

GY813 was notably more cytotoxic than Sorafenib in resistant glioma cell spheroids when cell viability was estimated by propidium iodide staining. This finding was in line with preliminary work in 2D cell cultures. This is a promising finding as the 3D culture model better reflects the tumour microenvironment than 2D cell viability assays. The capacity to disrupt tumour structure and the detection of dead cells in the hypoxic core of the spheroid, highlight the potential of GY813 to penetrate into the core of the tumour mass. It will be interesting to see if this holds true in animal models. In particular, the relative systemic toxicity of Sorafenib and GY813 will be a strong indicator of the therapeutic potential of GY813.

Future work can also be performed in spheroid heterocultures, whereby tumour cells are co-cultured with non-transformed cells to better reflect the tumour microenvironment. In this way, the selectivity of GY813 and Sorafenib toward cancer cells over non-transformed can be investigated in a 3D model, providing a more realistic analysis of compound selectivity.

5 Concluding Remarks

The work in this thesis highlights the potential of organic Se compounds as anticancer agents. As has previously been reported, the metabolism of supra-nutritional levels of redox active Se compounds clearly resulted in the generation of ROS and oxidative stress in pancreatic cancer cells. This ultimately accounted for their cytotoxicity and specificity toward K-Ras mutated cell lines, which possess a "maximised" basal level of antioxidant activity, leaving them vulnerable to treatment with oxidants, such as Se compounds.

In part 1 of this thesis, a thorough investigation of the cytotoxicity, mechanism of action and cell line-specific activity of commercially available organic Se compounds (MSA, SeC and MSC) was undertaken. MSA clearly emerged as both the most potent and selective compound toward K-Ras mutated pancreatic cancer lines, being more cytotoxic and inducing notably higher levels of oxidative stress in K-Ras mutated PSN1 cells than in K-Ras wild-type BxPC3 cells. Moreover, the selectivity of Se compounds toward PSN1 cells over BxPC3 cells could be explained by the difference in the capacity of cells to upregulate their antioxidant defence when facing treatment with redox active Se compounds. Specifically, BxPC3 cells demonstrated a high capacity for increasing the total activity across a range of critical antioxidant enzymes, namely TrxR, GR and GPx, while PSN1 cells did not. This finding is particularly interesting when considering the differences observed between the aberrant metabolism of cancer cells and that of normal cells. Due to the metabolic shift toward aerobic glycolysis, cancer cells produce high levels of ROS and, in turn, develop a critical capacity to scavenge ROS in order to sustain their uncontrolled growth. In principle, this leaves cancer cells more susceptible to treatment with oxidants than normal cells as their antioxidant defences are already maximised. Importantly, we observed that this principle holds true in practice, offering a therapeutic window for the use of oxidants as cancer treatments. Moreover, in our In Vivo mouse model, MSA was both a more potent anti-tumour agent and less toxic than selenite. From this, we can reaffirm the notion that organic Se compounds offer a comparable anti-tumour potential to selenite with lower systemic side-effects, which have hindered the advancement of the use of selenite in cancer therapy.

In the second part of this thesis, the efficacy of newly synthesised Se derivatives (GY811, GY812 and GY813) of therapeutically used TKIs (Imatinib, Dasatinib, Sorafenib) were examined in pancreatic cancer cells. Importantly, all Se derivatives showed a greater

cytotoxicity toward cancer cell lines than their parental compounds as well as a higher selectivity toward K-Ras mutated PSN1 and PANC1 cells than toward K-Ras wild-type BxPC3 cells and non-transformed HEK293 cells. Moreover, all Se derivatives induced higher levels of ROS, and presumably oxidative stress, than their parental compounds. Hence, the inclusion of a Se moiety in existing cancer therapeutics potentiates them for use as dual-action, multi-targeting compounds, that serve both as oxidants and retain their parental tyrosine kinase inhibitory action. Importantly, this finding extended beyond 2D cell culture models and was consistent in 3D spheroid cultures. Ultimately, the findings in this study pave the way for the future of use of many more Se derivatives of existing chemotherapeutic agents, especially if they continue to increase the potency and selectivity of parental compounds toward tumour cells.

In the future, the use of both naturally existing Se compounds and novel Se derivatives should continue to receive attention in the search for more effective anti-tumour agents. Their great potential for specifically targeting tumour cells with low system toxicity will be focal points of upcoming research. Since both the metabolism of Se typically has implications on redox systems and cancer cells possess a metabolic susceptibility to redox homeostasis, the potential for Se compounds as therapeutic agents extends to a wide range of different types of cancer cells.

6 References

1. Pillai, R., Uyehara-Lock, J. H. & Bellinger, F. P. Selenium and selenoprotein function in brain disorders. *IUBMB Life* **66,** 229–239 (2014).

2. Chen, J. & Berry, M. J. Selenium and selenoproteins in the brain and brain diseases. *Journal of Neurochemistry* **86,** 1–12 (2003).

3. Kryukov, G. V *et al.* Characterization of mammalian selenoproteomes. *Science* **300,** 1439–1443 (2003).

4. Lee, S. R. *et al.* Mammalian thioredoxin reductase: oxidation of the C-terminal cysteine/selenocysteine active site forms a thioselenide, and replacement of selenium with sulfur markedly reduces catalytic activity. *Proc. Natl. Acad. Sci. U. S. A.* **97,** 2521–2526 (2000).

5. Stadtman, T. C. Selenocysteine. *Annu. Rev. Biochem.* **65,** 83–100 (1996).

6. Lee, B. J., Worland, P. J., Davis, J. N., Stadtman, T. C. & Hatfield, D. L. Identification of a selenocysteyl-tRNA(Ser) in mammalian cells that recognizes the nonsense codon, UGA. *J. Biol. Chem.* **264,** 9724–9727 (1989).

7. Berry, M. J. *et al.* Recognition of UGA as a selenocysteine codon in type I deiodinase requires sequences in the 3' untranslated region. *Nature* **353,** 273–6 (1991).

8. Berry, M. J., Banu, L., Harney, J. W. & Larsen, P. R. Functional characterization of the eukaryotic SECIS elements which direct selenocysteine insertion at UGA codons. *EMBO J.* **12,** 3315–22 (1993).

9. Shen, Q., Chu, F. F. & Newburger, P. E. Sequences in the 3'-untranslated region of the human cellular glutathione peroxidase gene are necessary and sufficient for selenocysteine incorporation at the UGA codon. *J. Biol. Chem.* **268,** 11463–11469 (1993).

10. Xu, X. M. *et al.* Biosynthesis of selenocysteine on its tRNA in eukaryotes. *PLoS Biol.* **5,** 0096–0105 (2007).

11. Rayman, M. P., Infante, H. G. & Sargent, M. Food-chain selenium and human health: spotlight on speciation. *Br. J. Nutr.* **100,** 238–253 (2008).

12. Pitts, M. W., Byrns, C. N., Ogawa-Wong, A. N., Kremer, P. & Berry, M. J. Selenoproteins in Nervous System Development and Function. *Biol. Trace Elem. Res.* **161,** 231–245 (2014).

13. Fernandes, A. P. & Gandin, V. Selenium compounds as therapeutic agents in cancer. *Biochimica et Biophysica Acta - General Subjects* **1850,** 1642–1660 (2015).

14. Björnstedt, M., Kumar, S. & Holmgren, A. Selenodiglutathione is a highly efficient oxidant of reduced thioredoxin and a substrate for mammalian thioredoxin reductase. *J. Biol. Chem.* **267,** 8030–8034 (1992).

15. Wallenberg, M., Olm, E., Hebert, C., Björnstedt, M. & Fernandes, A. P. Selenium compounds are substrates for glutaredoxins: a novel pathway for selenium metabolism and a potential mechanism for selenium-mediated cytotoxicity. *Biochem. J.* **429,** 85–93 (2010).

16. Hughes, D. J. *et al.* Selenium status is associated with colorectal cancer risk in the European prospective investigation of cancer and nutrition cohort. *Int. J. Cancer* **136,** 1149–1161 (2015).

17. Rayman, M. P. Selenium and human health. *The Lancet* **379,** 1256–1268 (2012).

18. Jung, H. J. & Seo, Y. R. Current issues of selenium in cancer chemoprevention. *BioFactors* **36,** 153–158 (2010).

19. Puspitasari, I. M. *et al.* Updates on clinical studies of selenium supplementation in radiotherapy. *Radiat. Oncol.* **9,** 125 (2014).

20. Tan, Q. *et al.* Augmented antitumor effects of combination therapy of cisplatin with ethaselen as a novel thioredoxin reductase inhibitor on human A549 cell in vivo. *Invest. New Drugs* **28,** 205–215 (2010).

21. Yakubov, E., Buchfelder, M., Eyüpoglu, I. Y. & Savaskan, N. E. Selenium Action in Neuro-Oncology. *Biol. Trace Elem. Res.* **161,** 246–254 (2014).

22. Weekley, C. M. & Harris, H. H. Which form is that? The importance of selenium speciation and metabolism in the prevention and treatment of disease. *Chem. Soc. Rev.* **42,** 8870–94 (2013).

23. Valdiglesias, V., Pásaro, E., Méndez, J. & Laffon, B. In vitro evaluation of selenium genotoxic, cytotoxic, and protective effects: A review. *Archives of Toxicology* **84,** 337–351 (2010).

24. Chen, Y.-C., Prabhu, K. S., Das, A. & Mastro, A. M. Dietary selenium supplementation modifies breast tumor growth and metastasis. *Int. J. Cancer* **133,** 2054–64 (2013).

25. Cairns, R. A., Harris, I., Mccracken, S. & Mak, T. W. Cancer cell metabolism. *Cold Spring Harb. Symp. Quant. Biol.* **76,** 299–311 (2011).

26. Gorrini, C., Harris, I. S. & Mak, T. W. Modulation of oxidative stress as an anticancer strategy. *Nat. Rev. Drug Discov.* **12,** 931–947 (2013).

27. Diehn, M. *et al.* Association of reactive oxygen species levels and radioresistance in cancer stem cells. *Nature* **458,** 780–783 (2009).

28. Rooprai, H. K. *et al.* Inhibition of invasion and induction of apoptosis by selenium in human malignant brain tumour cells in vitro. *Int. J. Oncol.* **30,** 1263–1271 (2007).

29. Nilsonne, G. *et al.* Selenite induces apoptosis in sarcomatoid malignant mesothelioma cells through oxidative stress. *Free Radic. Biol. Med.* **41,** 874–885 (2006).

30. Husbeck, B., Nonn, L., Peehl, D. M. & Knox, S. J. Tumor-selective killing by selenite in patient-matched pairs of normal and malignant prostate cells. *Prostate* **66,** 218–225

(2006).

31. Jariwalla, R. J., Gangapurkar, B. & Nakamura, D. Differential sensitivity of various human tumour-derived cell types to apoptosis by organic derivatives of selenium. *Br. J. Nutr.* **101,** 182–9 (2009).

32. Gammelgaard, B., Jackson, M. I. & Gabel-Jensen, C. Surveying selenium speciation from soil to cell-forms and transformations. *Analytical and Bioanalytical Chemistry* **399,** 1743–1763 (2011).

33. Ganther, H. E. Selenium metabolism, selenoproteins and mechanisms of cancer prevention: Complexities with thioredoxin reductase. *Carcinogenesis* **20,** 1657–1666 (1999).

34. Pantano, C., Reynaert, N. L., van der Vliet, A. & Janssen-Heininger, Y. M. W. Redox-sensitive kinases of the nuclear factor-kappaB signaling pathway. *Antioxid. Redox Signal.* **8,** 1791–806 (2006).

35. Zou, Y. *et al.* The JNK signaling pathway is involved in sodium-selenite-induced apoptosis mediated by reactive oxygen in HepG2 cells. *Cancer Biol. Ther.* **7,** 689–96 (2008).

36. Husbeck, B., Bhattacharyya, R. S., Feldman, D. & Knox, S. J. Inhibition of androgen receptor signaling by selenite and methylseleninic acid in prostate cancer cells: two distinct mechanisms of action. *Mol. Cancer Ther.* **5,** 2078–85 (2006).

37. Ranawat, P. & Bansal, M. P. Decreased glutathione levels potentiate the apoptotic efficacy of selenium: Possible involvement of p38 and JNK MAPKs - In vitro studies. *Mol. Cell. Biochem.* **309,** 21–32 (2008).

38. Flohé, L., Brigelius-Flohé, R., Saliou, C., Traber, M. G. & Packer, L. Redox regulation of NF-kappa B activation. *Free Radic. Biol. Med.* **22,** 1115–1126 (1997).

39. Zorn, M., Ihling, C. H., Golbik, R., Sawers, R. G. & Sinz, A. Selective selC-Independent Selenocysteine Incorporation into Formate Dehydrogenases. *PLoS One* **8,** (2013).

40. Wallenberg, M. *et al.* Selenium induces a multi-targeted cell death process in addition to ROS formation. *J. Cell. Mol. Med.* **18,** 671–684 (2014).

41. Lu, J., Kaeck, M., Jiang, C., Wilson, A. C. & Thompson, H. J. Selenite induction of DNA strand breaks and apoptosis in mouse leukemic L1210 cells. *Biochem Pharmacol* **47,** 1531–1535 (1994).

42. More, A. & Cavalieri, R. R. Sodium Selenite Se 75 A More Specific Agent for Scanning Tumors. *JAMA* **206,** 591–595 (1968).

43. Ganyc, D. & Self, W. T. High affinity selenium uptake in a keratinocyte model. *FEBS Lett.* **582,** 299–304 (2008).

44. Lewerenz, J. *et al.* The cystine/glutamate antiporter system x(c)(-) in health and disease: from molecular mechanisms to novel therapeutic opportunities. *Antioxid. Redox Signal.* **18,** 522–55 (2013).

45. Olm, E. *et al.* Extracellular thiol-assisted selenium uptake dependent on the x(c)-cystine transporter explains the cancer-specific cytotoxicity of selenite. *Proc. Natl. Acad. Sci. U. S. A.* **106,** 11400–11405 (2009).

46. Labunskyy, V. M., Hatfield, D. L. & Gladyshev, V. N. Selenoproteins: Molecular Pathways and Physiological Roles. *Physiol. Rev.* **94,** 739–777 (2014).

47. Björkhem-Bergman-Bergman, Linda Jönsson, K. *et al.* Drug-resistant human lung cancer cells are more sensitive to selenium cytotoxicity: Effects on thioredoxin reductase and glutathione reductase. *Biochem. Pharmacol.* **63,** 1875–1884 (2002).

48. Selenius, M., Fernandes, A. P., Brodin, O., Bjornstedt, M. & Rundlof, A. K. Treatment of lung cancer cells with cytotoxic levels of sodium selenite: effects on the thioredoxin system. *Biochem. Pharmacol.* **75,** 2092–2099 (2008).

49. Xiang, N., Zhao, R. & Zhong, W. Sodium selenite induces apoptosis by generation of superoxide via the mitochondrial-dependent pathway in human prostate cancer cells. *Cancer Chemother. Pharmacol.* **63,** 351–362 (2009).

50. Fu, L., Liu, Q., Shen, L. & Wang, Y. Proteomic study on sodium selenite-induced apoptosis of human cervical cancer HeLa cells. *J. Trace Elem. Med. Biol.* **25,** 130–7 (2011).

51. Rigobello, M. P. *et al.* Treatment of human cancer cells with selenite or tellurite in combination with auranofin enhances cell death due to redox shift. *Free Radic. Biol. Med.* **47,** 710–721 (2009).

52. Králová, V., Benešová, S., Červinka, M. & Rudolf, E. Selenite-induced apoptosis and autophagy in colon cancer cells. *Toxicol. Vitr.* **26,** 258–268 (2012).

53. Li, Z., Meng, J., Xu, T.-J., Qin, X.-Y. & Zhou, X.-D. Sodium selenite induces apoptosis in colon cancer cells via Bax-dependent mitochondrial pathway. *Eur. Rev. Med. Pharmacol. Sci.* **17,** 2166–71 (2013).

54. Olm, E. *et al.* Selenite is a potent cytotoxic agent for human primary AML cells. *Cancer Lett.* **282,** 116–123 (2009).

55. Philchenkov, A., Zavelevich, M., Khranovskaya, N. & Surai, P. Comparative analysis of apoptosis induction by selenium compounds in human lymphoblastic leukemia MT-4 cells. *Exp. Oncol.* **29,** 257–261 (2007).

56. Celik, H. A. *et al.* Biochemical and morphological characteristics of selenite-induced apoptosis in human hepatoma Hep G2 cells. *Biol. Trace Elem. Res.* **99,** 27–40 (2004).

57. Bandura, L., Drukala, J., Wolnicka-Glubisz, A., Björnstedt, M. & Korohoda, W. Differential effects of selenite and selenate on human melanocytes, keratinocytes, and melanoma cells. *Biochem. Cell Biol.* **83,** 196–211 (2005).

58. Freitas, M., Alves, V., Sarmento-Ribeiro, A. B. & Mota-Pinto, A. Combined effect of sodium selenite and docetaxel on PC3 metastatic prostate cancer cell line. *Biochem Biophys Res Commun* **408,** 713–719 (2011).

59. Schroeder, C. P. *et al.* Effect of selenite combined with chemotherapeutic agents on the proliferation of human carcinoma cell lines. *Biol. Trace Elem. Res.* **99,** 17–25 (2004).

60. Rudolf, E., Radocha, J., Cervinka, M. & Cerman, J. Combined effect of sodium selenite and campthotecin on cervical carcinoma cells. *Neoplasma* **51,** 127–135 (2004).

61. Jönsson-Videsäter, K. *et al.* Selenite-induced apoptosis in doxorubicin-resistant cells and effects on the thioredoxin system. *Biochem. Pharmacol.* **67,** 513–522 (2004).

62. Tobe, T., Ueda, K., Ando, M., Okamoto, Y. & Kojima, N. Thiol-mediated multiple mechanisms centered on selenodiglutathione determine selenium cytotoxicity against MCF-7 cancer cells. *JBIC J. Biol. Inorg. Chem.* **20,** 687–694 (2015).

63. Lanfear, J., Fleming, J., Wu, L., Webster, G. & Harrison, P. R. The selenium metabolite selenodiglutathione induces p and apoptosis: Relevance to the chemopreventive effects of selenium? *Carcinogenesis* **15,** 1387–1392 (1994).

64. Cho, D. Y., Jung, U. & Chung, A. S. Induction of apoptosis by selenite and selenodiglutathione in HL-60 cells: correlation with cytotoxicity. *Biochem Mol Biol Int* **47,** 781–793 (1999).

65. Wu, L., Lanfear, J. & Harrison, P. R. The selenium metabolite selenodiglutathione induces cell death by a mechanism distinct from H2O2 toxicity. *Carcinogenesis* **16,** 1579–1584 (1995).

66. Ghose, A., Fleming, J., El-Bayoumy, K. & Harrison, P. R. Enhanced sensitivity of human oral carcinomas to induction of apoptosis by selenium compounds: Involvement of mitogen-activated protein kinase and Fas pathways. *Cancer Res.* **61,** 7479–7487 (2001).

67. Redman, C. *et al.* Inhibitory effect of selenomethionine on the growth of three selected human tumor cell lines. *Cancer Lett.* **125,** 103–10 (1998).

68. Baines, A. *et al.* Selenomethionine inhibits growth and suppresses cyclooxygenase-2 (COX-2) protein expression in human colon cancer cell lines. *Cancer Biol. Ther.* **1,** 370–4 (2002).

69. Suzuki, M. ., Endo, M. . b, Shinohara, F. ., Echigo, S. . & Rikiishi, H. . Differential apoptotic response of human cancer cells to organoselenium compounds. *Cancer Chemother. Pharmacol.* **66,** 475–484 (2010).

70. Pinto, J. T. *et al.* Differential effects of naturally occurring and synthetic organoselenium compounds on biomarkers in androgen responsive and androgen independent human prostate carcinoma cells. *Int. J. Cancer* **120,** 1410–1417 (2007).

71. Yang, Y. *et al.* The anticancer effects of sodium selenite and selenomethionine on human colorectal carcinoma cell lines in nude mice. *Oncol Res* **18,** 1–8 (2009).

72. Poerschke, R. L. & Moos, P. J. Thioredoxin reductase 1 knockdown enhances selenazolidine cytotoxicity in human lung cancer cells via mitochondrial dysfunction.

Biochem. Pharmacol. **81,** 211–221 (2011).

73. Chen, T. & Wong, Y. S. Selenocystine induces reactive oxygen species-mediated apoptosis in human cancer cells. *Biomed. Pharmacother.* **63,** 105–113 (2009).

74. Chen, T. & Wong, Y. S. Selenocystine induces apoptosis of A375 human melanoma cells by activating ROS-mediated mitochondrial pathway and p53 phosphorylation. *Cell. Mol. Life Sci.* **65,** 2763–2775 (2008).

75. Chen, T. & Wong, Y. S. Selenocystine induces caspase-independent apoptosis in MCF-7 human breast carcinoma cells with involvement of p53 phosphorylation and reactive oxygen species generation. *Int. J. Biochem. Cell Biol.* **41,** 666–676 (2009).

76. Fan, C. *et al.* Enhancement of auranofin-induced lung cancer cell apoptosis by selenocystine, a natural inhibitor of TrxR1 in vitro and in vivo. *Cell Death Dis.* **5,** e1191 (2014).

77. Liu, C. *et al.* Enhancement of Auranofin-Induced Apoptosis in MCF-7 Human Breast Cells by Selenocystine, a Synergistic Inhibitor of Thioredoxin Reductase. *PLoS One* **8,** (2013).

78. Jiang, C., Wang, Z., Ganther, H. & Lü, J. Distinct effects of methylseleninic acid versus selenite on apoptosis, cell cycle, and protein kinase pathways in DU145 human prostate cancer cells. *Mol. Cancer Ther.* **1,** 1059–1066 (2002).

79. Jiang, C., Wang, Z., Ganther, H. & Lu, J. Caspases as key executors of methyl selenium-induced apoptosis (anoikis) of DU-145 prostate cancer cells. *Cancer Res.* **61,** 3062–3070 (2001).

80. Tarrado-Castellarnau, M. *et al.* Methylseleninic acid promotes antitumour effects via nuclear FOXO3a translocation through Akt inhibition. *Pharmacol. Res.* **102,** 218–234 (2015).

81. Poerschke, R. L., Franklin, M. R. & Moos, P. J. Modulation of redox status in human lung cell lines by organoselenocompounds: Selenazolidines, selenomethionine, and methylseleninic acid. *Toxicol. Vitr.* **22,** 1761–1767 (2008).

82. Li, G.-X. ., Hu, H. ., Jiang, C. ., Schuster, T. . & Lü, J. . b. Differential involvement of reactive oxygen species in apoptosis induced by two classes of selenium compounds in human prostate cancer cells. *Int. J. Cancer* **120,** 2034–2043 (2007).

83. Shigemi, Z. *et al.* Methylseleninic acid and sodium selenite induce severe (ER) stress and subsequent apoptosis through (UPR) activation in (PEL) cells. *Chem. Biol. Interact.* **266,** 28–37 (2017).

84. Guo, C.-H., Hsia, S., Shih, M.-Y., Hsieh, F.-C. & Chen, P.-C. Effects of Selenium Yeast on Oxidative Stress, Growth Inhibition, and Apoptosis in Human Breast Cancer Cells. *Int. J. Med. Sci.* **12,** 748–758 (2015).

85. Wang, L. *et al.* Methyl-selenium compounds inhibit prostate carcinogenesis in the transgenic adenocarcinoma of mouse prostate model with survival benefit. *Cancer*

Prev. Res. **2,** 484–495 (2009).

86. Schröterová, L. *et al.* Antiproliferative effects of selenium compounds in colon cancer cells: Comparison of different cytotoxicity assays. *Toxicol. Vitr.* **23,** 1406–1411 (2009).

87. Bhattacharya, A. *et al.* Tumor vascular maturation and improved drug delivery induced by methylselenocysteine leads to therapeutic synergy with anticancer drugs. *Clin. Cancer Res.* **14,** 3926–3932 (2008).

88. Bhattacharya, A. Methylselenocysteine: a Promising Antiangiogenic Agent for Overcomimng Drug Delivery arriers in Solis Malignancies for Therapeutic Synergy with Anticancer Drugs. *Expert Opin Drug Deliv* **8,** 749–763 (2011).

89. Li, Z. *et al.* Combination of methylselenocysteine with tamoxifen inhibits MCF-7 breast cancer xenografts in nude mice through elevated apoptosis and reduced angiogenesis. *Breast Cancer Res. Treat.* **118,** 33–43 (2009).

90. Cao, S., Durrani, F. A., Tóth, K. & Rustum, Y. M. Se-methylselenocysteine offers selective protection against toxicity and potentiates the antitumour activity of anticancer drugs in preclinical animal models. *Br. J. Cancer* **110,** 1733–43 (2014).

91. Duckett, D. R. & Cameron, M. D. Metabolism considerations for kinase inhibitors in cancer treatment. *Expert Opin. Drug Metab. Toxicol.* **6,** 1175–1193 (2010).

92. O'Hare, T. *et al.* In vitro activity of Bcr-Abl inhibitors AMN107 and BMS-354825 against clinically relevant imatinib-resistant Abl kinase domain mutants. *Cancer Res.* **65,** 4500–4505 (2005).

93. Karaman, M. W. *et al.* A quantitative analysis of kinase inhibitor selectivity. *Nat. Biotechnol.* **26,** 127–132 (2008).

94. Ziogas, I. A. & Tsoulfas, G. Evolving role of Sorafenib in the management of hepatocellular carcinoma. *World J. Clin. Oncol.* **8,** 203 (2017).

95. Bruix, J. *et al.* Regorafenib for patients with hepatocellular carcinoma who progressed on sorafenib treatment (RESORCE): a randomised, double-blind, placebo-controlled, phase 3 trial. *Lancet* **389,** 56–66 (2017).

96. Cairns, R. a, Harris, I. S. & Mak, T. W. Regulation of cancer cell metabolism. *Nat. Rev. Cancer* **11,** 85–95 (2011).

97. Pliarchopoulou, K. & Pectasides, D. Pancreatic cancer: Current and future treatment strategies. *Cancer Treatment Reviews* **35,** 431–436 (2009).

98. Pasca di Magliano, M. & Logsdon, C. D. Roles for KRAS in Pancreatic Tumor Development and Progression. *Gastroenterology* **144,** 1220–1229 (2014).

99. Logsdon, C. D. & Lu, W. The significance of ras activity in pancreatic cancer initiation. *International Journal of Biological Sciences* **12,** 338–346 (2016).

100. Glasauer, A. & Chandel, N. S. Targeting antioxidants for cancer therapy. *Biochemical Pharmacology* **92,** 90–101 (2014).

101. Shaw, A. T. *et al.* Selective killing of K-ras mutant cancer cells by small molecule inducers of oxidative stress. *Proc. Natl. Acad. Sci. U. S. A.* **108,** 8773–8 (2011).

102. Misra, S., Boylan, M., Selvam, A., Spallholz, J. E. & Björnstedt, M. Redox-active selenium compounds - from toxicity and cell death to cancer treatment. *Nutrients* **7,** 3536–56 (2015).

103. Ip, C., Thompson, H. J., Zhu, Z. & Ganther, H. E. In vitro and in vivo studies of methylseleninic acid: Evidence that a monomethylated selenium metabolite is critical for cancer chemoprevention. *Cancer Res.* **60,** 2882–2886 (2000).

104. Sayin, V. I. *et al.* Antioxidants accelerate lung cancer progression in mice. *Sci. Transl. Med.* **6,** 221ra15 (2014).

105. Le Gal, K. *et al.* Antioxidants can increase melanoma metastasis in mice. *Sci. Transl. Med.* **7,** 308re8-308re8 (2015).

106. Piskounova, E. *et al.* Oxidative stress inhibits distant metastasis by human melanoma cells. *Nature* **527,** 186–91 (2015).